Journal of Quantitative Spectroscopy & Radiative Transfer 182 (2016) 199–218

Contents lists available at ScienceDirect

Journal of Quantitative Spectroscopy & Radiative Transfer

journal homepage: www.elsevier.com/locate/jqsrt

First high resolution ro-vibrational study of the (0200), (0101) and (0002) vibrational states of $^{M}GeH_4$ ($M=76,74$)

O.N. Ulenikov [a,*], O.V. Gromova [a], E.S. Bekhtereva [a], N.I. Raspopova [a], A.L. Fomchenko [a], P.G. Sennikov [b], M.A. Koshelev [b,c], I.A. Velmuzhova [b], A.P. Velmuzhov [b]

[a] Institute of Physics and Technology, National Research Tomsk Polytechnic University, Tomsk 634050, Russia
[b] G.G. Devyatykh Institute of Chemistry of High Purity Substances, Russian Academy of Sciences, 603950 Nizhny Novgorod, Russia
[c] Institute of Applied Physics, Russian Academy of Sciences, 603950 Nizhny Novgorod, Russia

ARTICLE INFO

Article history:
Received 14 April 2016
Received in revised form
12 May 2016
Accepted 12 May 2016
Available online 26 May 2016

Keywords:
The (0200)/(0101)/(0002) interacting states of GeH_4
High resolution spectrum of GeH_4
The spectroscopic parameters

ABSTRACT

The infrared spectra of GeH_4 (88.1% of $^{76}GeH_4$, 11.5% of $^{74}GeH_4$, and a minor amounts of three other stable isotopic species in the sample) were measured in the region of 1450–2000 cm^{-1} with a Bruker IFS 125HR Fourier transform interferometer (Nizhny Novgorod, Russia) and analyzed. 2254 transitions with $J^{max}=19$ were assigned for the first time to the bands $2\nu_4(F_2)$, $2\nu_4(E)$, $\nu_2+\nu_4(F_2)$, $\nu_2+\nu_4(F_1)$, $2\nu_2(A_1)$ and $2\nu_2(E)$ of the $^{76}GeH_4$ isotopologue. Numerous "hot" Dyad–Pentad transitions also were recorded and assigned for the first time in the region of 700–1080 cm^{-1} (in general, about 1000 transitions). Rotational, centrifugal distortion, tetrahedral splitting, and interaction parameters for the $(0002,F_2)$, $(0002,E)$, $(0002,A_1)$, $(0101,F_2)$, $(0101,F_1)$, $(0200,A_1)$ and $(0200,E)$ vibrational states were determined from the fit of experimental line positions. The obtained set of parameters reproduces the initial experimental data with accuracy close to experimental uncertainties. Results of the analogous analysis of the $^{74}GeH_4$ isotopologue (the number of assigned transitions is 309 "cold" and 99 "hot" ones) are presented also. Obtained from the weighted fit set of spectroscopic parameters of the effective Hamiltonian reproduces the initial experimental data with the d_{rms} better than 3×10^{-4} cm^{-1}.

1. Introduction

Knowledge of internal properties of the germane molecule is very important for numerous both pure scientific and applied problems of physics, chemistry, astrophysics, industry, etc. Germane is one of the important components of atmospheres of giant gas-planet such as Jupiter and Saturn [1–4], and its presence should be taken into account at studies of the compositions and chemistry of their atmospheres. In particular, in atmospheres of Jupiter and Saturn germane was detected at abundances orders of magnitude greater than their thermochemical equilibrium values in the upper tropospheres [5]. Germane in a natural isotopic composition is used for producing high-purity germanium. On that basis various physical devices (e.g., high-sensitivity detectors of nuclear radiation) are manufactured [6]. Germane enriched by ^{76}Ge up to 88% can be used as starting substance for production of high purity single-crystal ^{76}Ge which, in its turn, can be used as a source of a double beta decay of its nuclei and, at the same time, as a detector of this process, Ref. [7]. Because of all of these reasons, laboratory investigations of high resolution spectra of germane are interesting and important.

Germane in a natural isotopic composition produces complex infrared spectra, first of all because of existence of

* Corresponding author.
E-mail address: Ulenikov@mail.ru (O.N. Ulenikov).

http://dx.doi.org/10.1016/j.jqsrt.2016.05.014
0022-4073/

Table 1
Experimental setup for the Dyad–Pentad regions of the infrared spectrum of $^{M}GeH_4$ ($M = 74, 76$).

Spectr.	Wavelength range (cm^{-1})	Resolution (cm^{-1})	Measuring time (h)	No. of scans	Source	Detector	Beam-splitter	Opt. path-length (m)	Aperture (mm)	Temp. (°C)	Pressure (Torr)	Calibr. gas
I	700–1080	0.003	33.5	1000	Globar	MCT	KBr	0.20	1.7	21.1	0.4	OCS
II	700–1080	0.003	26.8	800	Globar	MCT	KBr	0.20	1.7	23.9	10	OCS
III	1580–2250	0.003	33.5	1050	Globar	MCT	KBr	0.20	1.3	24.5	4	H_2O
IV	1580–2250	0.003	35.2	1050	Globar	MCT	KBr	2.25	1.5	21.4	3.5	H_2O
V	1800–4500	0.003	35.2	1050	Globar	InSb	KBr	3.75	1.0	22.6	3	H_2O

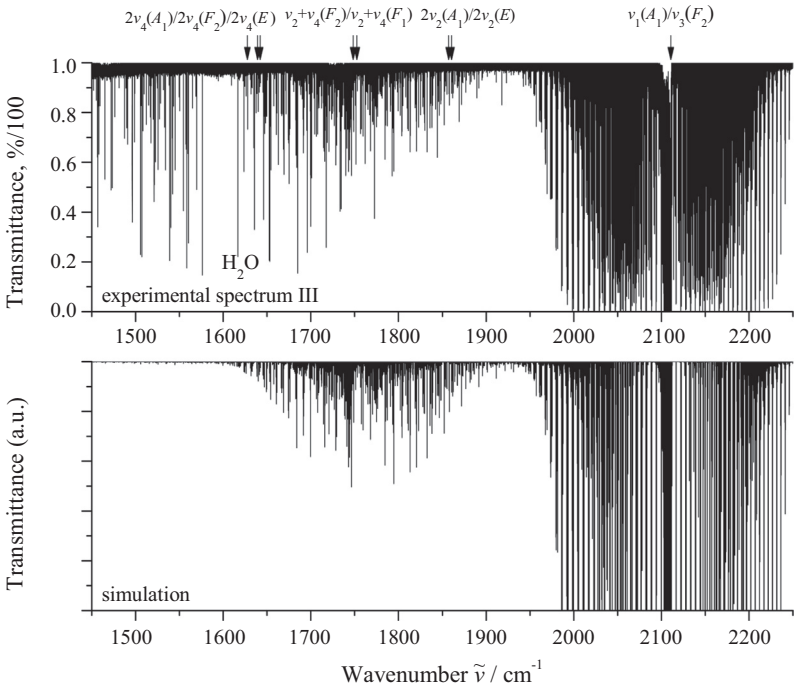

Fig. 1. Survey spectra of $^{76}GeH_4$ and $^{74}GeH_4$ in the Pentad region. The top trace presents the experimental spectrum III. Experimental conditions: absorption path length is 2.25 m; room temperature; number of scans is 1050; sample pressure is 3.5 Torr. The bottom trace presents, for illustration, simulated spectrum (see text for details).

five stable isotopologues with mass numbers 70 (20.55%), 72 (27.37%), 73 (7.67%), 74 (36.74%), and 76 (7.67%). Additional complexity of the germane spectra arises from the presence of very strong resonance interactions between its ro-vibrational bands. Spectra of different $^{M}GeH_4$ ($M = 70, 72, 73, 74, 76$) isotopologues of germane were the objects of study during many years. In this case, up to 1972 the spectra were recorded with a low or medium resolution. High resolution spectra of germane started being studied in 1973 (see, Refs. [8–33]). In 1973, Oka with co-authors extensively studied pure rotational spectra of the XH_4 (T_d symmetry) molecules (X=C, Ge, Si) by the method of infrared-microwave double resonance [8–12]. The first high resolution infrared spectrum of germane (ν_3 and $2\nu_3$ bands of all five isotopologues) was considered in [13]. High resolution spectra of highly excited overtone stretching bands of germane were extensively discussed in papers of Zhu with co-authors [25–31], in the frame of the local mode model. Concerning the bending bands, only fundamentals ν_2 and ν_4 were analyzed earlier with high resolution [18,19,22,23,32]. To our knowledge, the bands which correspond to double excitations of deformational vibrations were not discussed in the literature at all.

In this paper we present the results of analysis of the high resolution Fourier transformed spectra of $^{M}GeH_4$ ($M = 74, 76$) in the region of 1450–2000 cm^{-1} where the $2\nu_4(F_2)$, $2\nu_4(E)$, $2\nu_4(A_1)$, $\nu_2+\nu_4(F_2)$, $\nu_2+\nu_4(F_1)$, $2\nu_2(A_1)$ and $2\nu_2(E)$ bands are located. Additionally, "hot" Dyad–Pentad[1] transitions also were recorded and assigned for the first time in the region of 700–1080 cm^{-1}. The experimental details are given in Section 2. Description of the spectra and assignment of transitions are discussed in Section 3. Section

[1] Here and further in this paper, in spite of the fact that the ν_1 and ν_3 bands of GeH_4 are more or less isolated from the $2\nu_2$, $\nu_2+\nu_4$, and $2\nu_4$ bands, for the shortness, we will use the name "Pentad" for the notation of the set of bands $2\nu_2$, $\nu_2+\nu_4$, $2\nu_4$, ν_1 and ν_3, as well as the name "Dyad" for the notation of the set of bands ν_2 and ν_4.

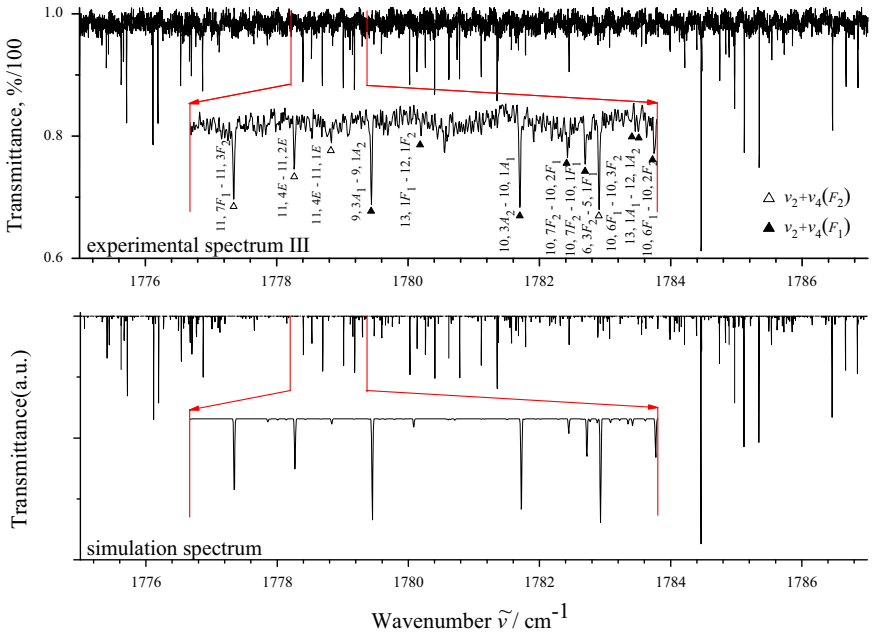

Fig. 2. Small portion (top trace) of high resolution spectrum of $^{76}GeH_4$ (weak lines of $^{74}GeH_4$ are not seen in this part of the spectrum) in the region of the Q/R-branches of the $\nu_2+\nu_4$ band (for experimental condition, see footnote to Fig. 1). The bottom trace presents, for illustration, simulated spectrum (see text for details).

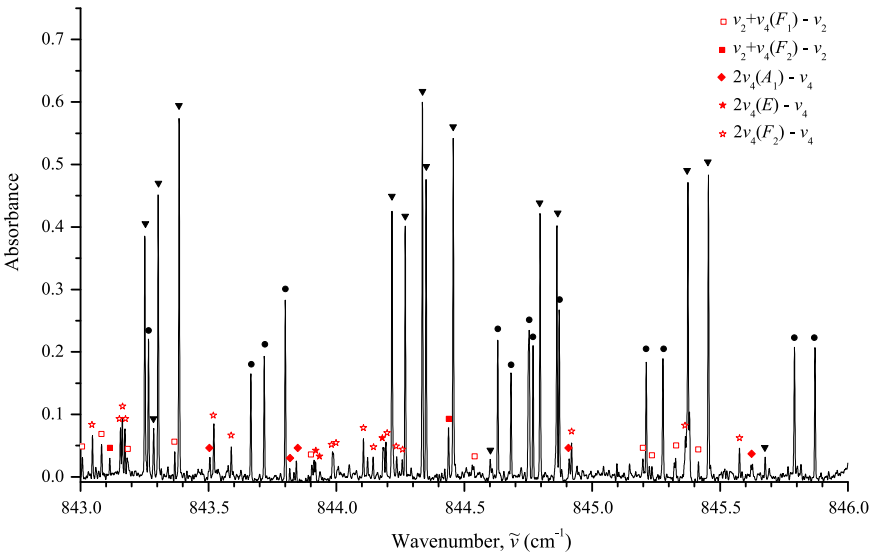

Fig. 3. Small portion of the high resolution spectrum of $^{76}GeH_4$ and $^{74}GeH_4$ in the region of the R-branch of the ν_4 band. Strong transitions belonging to the ν_4 band are marked by dark triangles and dark circles. Weak lines marked by open and red squares, dark rhombuses, dark and open stars belong to the "hot" Dyad–Pentad transitions. (For interpretation of the references to color in this figure caption, the reader is referred to the web version of this paper.)

4 presents briefly the theoretical background of our study. Results and discussion are presented in Section 5.

2. Experimental details

The high-resolution spectra of germane were recorded using a Bruker IFS 125HR Fourier transform spectrometer. The experimental details are summarized in Table 1. The enriched and purified gas sample of germane contained $^{76}GeH_4$ (88.1%), $^{74}GeH_4$ (11.5%), $^{73}GeH_4$ (0.07%), $^{72}GeH_4$ (0.17%) and $^{70}GeH_4$ (0.12%) isotopologues. In the current study two spectral ranges attracted our attention. The sample spectra in the 1450–2000 cm^{-1} range containing $2\nu_4$, $\nu_2+\nu_4$ and $2\nu_2$ vibrational bands were recorded at a few pressures using a multi-pass cell with 2.25 and 3.75 m optical path length. Some "hot" Dyad–Pentad vibrational bands were analyzed in the range 700–1080 cm^{-1} using the spectra from our earlier study [32]. For both ranges the resolution due to the maximum optical path difference was 0.003 cm^{-1} and the Norton–Beer (weak) apodization function was applied. The optical compartment of the spectrometer was evacuated by a mechanical pump down to 0.02 Torr (or less) and that pressure remained during the

Table 2
Statistical information for the $2\nu_2(A_1,E)$, $\nu_2+\nu_4(F_1,F_2)$ and $2\nu_4(A_1,E,F_2)$ bands of $^{76}GeH_4$ and $^{74}GeH_4$.

Band 1	Energy[a] (cm^{-1}) 2	J^{max} 3	N_{tr}[b] 4	N_l[c] 5	m_1[d] 6	m_2[d] 7	m_3[d] 8
$^{76}GeH_4$							
$2\nu_4(A_1)-\nu_4(F_2)$	1627.4950	11	76	29	76.3	17.1	6.6
$2\nu_4(F_2)-\nu_4(F_2)$		15	206				
$2\nu_4(F_2)$	1639.2570	15	100	189	66.3	19.6	14.1
$2\nu_4(E)-\nu_4(F_2)$		15	52				
$2\nu_4(E)$	1642.1422	13	28	43	65.0	20.0	15.0
$\nu_2+\nu_4(F_2)-\nu_4(F_2)$		16	119				
$\nu_2+\nu_4(F_2)-\nu_2(E)$		15	236				
$\nu_2+\nu_4(F_2)$	1748.3962	19	793	401	61.1	27.4	11.5
$\nu_2+\nu_4(F_1)-\nu_4(F_2)$		15	45				
$\nu_2+\nu_4(F_1)-\nu_2(E)$		15	179				
$\nu_2+\nu_4(F_1)$	1752.5031	18	699	289	65.3	24.4	10.3
$2\nu_2(A_1)$	1857.2721	18	131	64	79.4	12.2	8.4
$2\nu_2(E)-\nu_2(E)$		17	81				
$2\nu_2(E)$	1860.6673	19	503	257	78.4	13.9	7.7
Total N_{tr} (cold bands)			2254				
Total N_{tr} (hot bands)			994				
Total N_l				1272			
d_{rms} (cold bands)	2.6×10^{-4} cm^{-1}						
d_{rms} (hot bands)	2.9×10^{-4} cm^{-1}						
$^{74}GeH_4$							
$\nu_2+\nu_4(F_2)-\nu_2(E)$		12	50				
$\nu_2+\nu_4(F_2)$	1748.7773	15	159	156	71.3	21.5	7.2
$\nu_2+\nu_4(F_1)-\nu_2(E)$		11	49				
$\nu_2+\nu_4(F_1)$	1752.8865	13	150	129	58.8	28.1	13.1
Total N_{tr} (cold bands)			309				
Total N_{tr} (hot bands)			99				
Total N_l				285			
d_{rms} (cold bands)	2.7×10^{-4} cm^{-1}						
d_{rms} (hot bands)	2.9×10^{-4} cm^{-1}						

[a] Value of the upper vibrational energy.
[b] N_{tr} is the number of assigned transitions.
[c] N_l is the number of obtained upper-state energies.
[d] Here $m_i=n_i/N_l\times100\%$ $(i=1,2,3)$; n_1, n_2, and n_3 are the numbers of upper-state energies for which the differences $\delta=E^{exp}-E^{calc}$ satisfy the conditions $\delta\le2\times10^{-4}$ cm^{-1}, 2×10^{-4} $cm^{-1}<\delta\le4\times10^{-4}$ cm^{-1}, and $\delta>4\times10^{-4}$ cm^{-1}.

experiment. The final spectra obtained by averaging 800–1050 scans (see Table 1) were calibrated using, respectively, about 200 and 400 most intense and isolated peaks of H_2O and OCS located in the studied wavelength range. Parameters of the calibration lines are tabulated in HITRAN database [34], and in NIST calibration tables [35]. After calibration the standard deviation of the difference between the measured and tabulated peak positions was less than 2×10^{-4} cm^{-1}.

3. Description of the spectra and assignment of transitions

To give the reader an impression about relative strengths of the stretching and bending bands of the entad, Fig. 1 presents the survey spectrum III. On that figure one can see clearly pronounced the $\nu_2+\nu_4$ band ($\nu_2+\nu_4(F_2)$ and $\nu_2+\nu_4(F_1)$ sub-bands) with the centers near 1750 cm^{-1} which is considerably weaker than the stretching ν_3 and ν_1 bands at the right side of Fig. 1. The $2\nu_4$ band with the center near 1640 cm^{-1} and the $2\nu_2$ band with the center near 1860 cm^{-1} are not seen against the band $\nu_2+\nu_4$. A small portion of the recorded high resolution spectrum III in the region of the Q/R-branch of the $\nu_2+\nu_4$ band is shown at the top of Fig. 2. Transitions assigned to the $^{76}GeH_4$ isotopologue are marked by open and dark triangles for the $\nu_2+\nu_4(F_2)$ and $\nu_2+\nu_4(F_1)$ sub-bands, respectively.

As was mentioned in the Introduction, some "hot" Dyad–Pentad vibrational bands were also analyzed. In this case, we used the earlier recorded spectra in the region of 700–1080 cm^{-1} which were discussed in Ref. [32]. Fig. 3 reproduces Fig. 2 from Ref. [32] on which transitions of the dyad have been marked by dark triangles and dark circles (as was assumed in Ref. [32], weak unassigned lines in Fig. 2 maybe belong to the "hot" Dyad–Pentad transitions). Assigned in the present study "hot" transitions of the "Dyad–Pentad" are marked in Fig. 3 by open and red squares, red rhombuses, red and open stars for the sub-bands $\nu_2+\nu_4(F_1)-\nu_2$, $\nu_2+\nu_4(F_2)-\nu_2$, $2\nu_4(A_1)-\nu_4$, $2\nu_4(E)-\nu_4$, and $2\nu_4(F_2)-\nu_4$, respectively.

The GeH_4 molecule is a spherical top with a symmetry isomorphic to the T_d point symmetry group. As a consequence, transitions in absorption are allowed only between

Table 3
Ro-vibrational term values for the $(0200, A_1)$ and $(0002, A_1)$ vibrational states of the $^{76}GeH_4$ molecule (in cm^{-1}).[a]

J	n	γ	$E(0200, A_1)$	δ	$E(0002, A_1)$	δ	J	n	γ	$E(0200, A_1)$	δ	$E(0002, A_1)$	δ	J	n	γ	$E(0200, A_1)$	δ	$E(0002, A_1)$	δ
1			2	3	4	5	1			2	3	4	5	1			2	3	4	5
3	1	A_2			1659.2440	−4	9	1	A_1	2105.7580	−2			12	1	A_1	2282.8031	1		
3	1	F_1			1659.3225	2	9	1	A_2	2106.7476	0	1864.1752	−2	12	2	A_1	2294.9935	0		
4	1	A_1			1680.4617	0	9	1	E	2105.4096	2			12	2	E	2286.8618	0		
4	1	E			1680.5233	0	9	1	F_1	2103.7530	1	1863.5555	0	12	2	F_1	2285.5466	−4		
4	1	F_1			1680.5217	−2	9	2	F_1	2105.4904	1	1864.8391	2	12	1	F_2	2286.9478	−2		
4	1	F_2			1680.4518	2	9	3	F_1	2106.3607	0			12	2	F_2	2285.5010	−2		
5	1	E			1706.9915	0	9	1	F_2	2103.7753	−2	1863.6352	1	13	1	A_1	2356.2823	−2		
5	2	F_1	1940.7040	2	1706.9088	0	9	2	F_2	2106.5642	1			13	1	A_2	2358.6011	−1		
5	1	F_2			1706.9605	−1	10	1	A_1	2160.9491	−1			13	1	F_1	2353.1952	3		
6	1	A_1	1974.0720	−3	1738.2897	0	10	1	A_2			1915.4244	−1	13	3	F_1	2357.8058	−1		
6	1	A_2			1738.5952	1	10	1	E			1915.3317	0	13	4	F_1	2367.2983	1		
6	1	E	1972.9846	−1	1738.4574	−1	10	2	E	2161.4586	1			13	1	F_2	2353.1962	2		
6	1	F_1			1738.5505	−7	10	1	F_1	2160.2014	1			14	1	A_1	2434.0527	−1		
6	1	F_2	1973.0217	−2	1738.4912	1	10	2	F_1	2161.2833	0			14	2	E	2445.0769	0		
6	2	F_2	1973.7679	5			10	1	F_2	2158.0824	5			14	3	F_2	2435.1034	0		
7	1	A_2	2012.1371	0			10	2	F_2	2160.0771	−9	1916.6293	−1	14	4	F_2	2445.1106	2		
7	1	E	2012.5048	−1			10	3	F_2	2161.7511	1			15	1	A_2	2513.7885	−1		
7	1	F_1	2011.2078	−3	1775.1038	0	11	1	A_2	2220.0717	0			15	2	A_2	2528.4825	3		
7	2	F_1	2012.7944	0	1775.1928	3	11	1	E	2220.1908	4			15	2	F_1	2528.3160	−1		
7	1	F_2	2011.2657	1	1775.2123	2	11	2	E	2222.0703	0			15	2	F_2	2513.7906	−8		
7	2	F_2	2012.3618	1			11	1	F_1	2217.7613	−5			15	3	F_2	2528.3698	1		
8	1	A_1	2054.7790	0	1816.7754	1	11	2	F_1	2221.2597	2			16	1	E	2617.0026	−2		
8	1	E			1816.9077	1	11	3	F_1	2222.1931	−1			16	3	F_1	2616.9795	−3		
8	1	F_1			1816.8690	2	11	1	F_2			1972.2082	−1	16	2	F_2	2617.2425	5		
8	2	F_1	2056.4079	1			11	2	F_2	2220.1469	1			17	2	E	2711.4125	3		
8	1	F_2	2056.1106	1	1817.1788	−1	11	3	F_2	2221.6348	0			18	2	A_2	2810.3644	−2		
8	2	F_2	2056.9945	2																

[a] In Table 3, δ is the difference $E^{exp.} - E^{calc.}$ in units of 10^{-4} cm^{-1}.

Table 4
Ro-vibrational term values for the $(0200, E)$ and $(0002, E)$ vibrational states of the $^{76}GeH_4$ molecule (in cm^{-1}).[a]

J	n	γ	$E(0200, E)$	δ	$E(0002, E)$	δ	J	n	γ	$E(0200, E)$	δ	$E(0002, E)$	δ	J	n	γ	$E(0200, E)$	δ	$E(0002, E)$	δ
1	2	3			4	5	1			2	3	4	5	1			2	3	4	5
1	1	F_2	1866.2275	3			8	2	F_2	2060.5979	−2	1881.5189	1	12	2	E	2292.9022	−3	2129.8433	−1
2	1	A_1	1877.2940	0			8	3	F_2	2061.4919	1			12	3	E	2296.1611	−1		
2	1	E	1877.3951	0			8	4	F_2	2063.5059	−1			12	4	E	2300.3902	1		
2	1	F_1	1877.3335	−2	1668.8080	−1	9	1	A_1	2112.0729	1			12	5	E	2301.2167	−1		
3	1	E	1894.0182	−3			9	1	A_2	2111.0846	−2			12	1	F_1	2287.9582	−3		
3	1	F_1	1893.9169	−2	1663.7049	0	9	1	E	2108.7396	1			12	2	F_1	2289.2511	1		
3	2	F_1	1894.1952	2			9	2	E	2111.9527	0			12	3	F_1	2294.7112	1		
3	1	F_2	1893.9791	−7			9	3	E	2114.3919	1			12	4	F_1	2295.8388	−2		
3	2	F_2	1894.1120	−1	1690.5009	0	9	1	F_1	2108.7830	1			12	5	F_1	2296.2677	−1		
4	1	A_1	1916.7749	−2	1685.0735	0	9	2	F_1	2110.4111	4	1935.7005	0	12	6	F_1	2300.3318	−1		
4	1	A_2	1916.4058	1	1673.4405	2	9	3	F_1	2112.0483	0			12	7	F_1	2301.1403	0		
4	1	E	1916.0428	0	1699.7238	1	9	4	F_1	2114.3794	−1			12	1	F_2	2287.7667	1		
4	2	E	1916.4417	1	1718.4860	1	9	5	F_1	2114.4340	−2			12	2	F_2	2289.3556	1		
4	1	F_1	1916.1541	1	1684.7616	1	9	1	F_2	2108.6702	0			12	3	F_2	2292.9009	−1		
4	2	F_1	1916.6334	−1	1699.8330	2	9	2	F_2	2110.5297	2			12	4	F_2	2294.5998	2		
4	1	F_2	1916.0660	0			9	3	F_2	2111.6318	0	1898.7448	−2	12	5	F_2	2295.9370	2		
4	2	F_2	1916.4270	1			9	4	F_2	2112.2814	0	1935.6255	1	12	6	F_2	2300.5609	0		
5	1	A_1	1943.7918	−1	1729.1802	3	9	5	F_2	2114.4881	−1			12	7	F_2	2301.2657	0		
5	1	A_2	1943.7214	0			10	1	A_1	2165.7699	3	1995.1701	3	13	1	A_1	2368.6412	−1		
5	1	E	1944.5294	−1			10	2	A_1	2171.0125	0			13	2	A_1	2374.7304	2		
5	1	F_1	1943.6916	−1			10	1	A_2	2168.1836	−1			13	1	A_2	2366.7189	0		
5	2	F_1	1944.1787	0	1729.0232	2	10	2	A_2	2171.0123	−3			13	2	A_2	2374.9630	1	2197.7500	−3
5	3	F_1	1944.9565	1	1751.2140	−3	10	1	E	2163.5340	0			13	1	E	2359.0063	0		
5	1	F_2	1943.6862	1	1711.1478	2	10	2	E	2165.8492	2	1995.0945	3	13	2	E	2360.2414	1	2197.1270	−6
5	2	F_2	1944.2947	0	1728.9087	0	10	3	E	2167.6557	2			13	3	E	2366.7964	−1		
5	3	F_2	1944.5951	0	1750.9331	0	10	4	E	2170.8197	−1			13	4	E	2368.2353	1		
6	1	A_1	1977.2597	0	1789.4136	1	10	1	F_1	2163.4812	1			13	5	E	2373.8137	0		
6	1	A_2	1978.2263	1			10	2	F_1	2165.8187	2	1954.1002	−6	13	1	F_1	2359.2894	−1		
6	1	E	1976.7692	1			10	3	F_1	2167.5173	1	1995.1199	−1	13	2	F_1	2360.2849	3		
6	2	E	1977.6882	1			10	4	F_1	2167.8662	1			13	3	F_1	2364.5912	−5		
6	3	E	1978.8386	−3	1789.0995	2	10	5	F_1	2170.9894	2			13	4	F_1	2368.5400	2		
6	1	F_1	1976.7911	1			10	1	F_2	2163.5943	0			13	5	F_1	2373.2828	−3		
6	2	F_1	1977.5338	1	1763.6695	5	10	2	F_2	2166.7590	2			13	6	F_1	2373.9087	−1		
6	3	F_1	1978.0490	0	1789.2178	2	10	3	F_2	2168.0057	0			13	7	F_1	2374.8275	0		
6	1	F_2	1976.8193	1			10	4	F_2	2170.7964	0			13	1	F_2	2357.9161	0		
6	2	F_2	1978.0619	3			10	5	F_2	2170.9905	−1			13	2	F_2	2358.8639	0	2197.2987	−4
6	3	F_2	1978.8144	−2			11	1	A_1	2223.6490	−1	2014.7523	0	13	3	F_2	2360.1788	−1		
7	1	A_1	2017.2151	1			11	2	A_1	2228.8061	−1			13	5	F_2	2366.7672	1		
7	1	A_2	2018.2867	0			11	1	A_2	2223.8130	0			13	6	F_2	2368.2228	2		
7	1	E	2015.3663	1			11	2	A_2	2232.8516	0			13	7	F_2	2368.4438	0		
7	2	E	2016.9632	1			11	1	E	2227.9239	1			13	8	F_2	2373.4260	−2		
7	1	F_1	2015.3720	−1			11	2	E	2229.2686	1			13	9	F_2	2374.9016	2		
7	2	F_1	2016.1402	1			11	3	E	2233.2439	−1			14	1	A_1	2436.5883	−3		
7	3	F_1	2017.1214	1	1832.7771	0	11	1	F_1	2223.7061	−1			14	2	A_1	2441.6849	−7		
7	4	F_1	2018.3949	1			11	2	F_1	2226.6324	3			14	3	A_1	2453.0489	0		
7	1	F_2	2015.3002	1			11	3	F_1	2228.0011	0			14	1	A_2	2436.4158	3		
7	2	F_2	2016.5371	1	1803.4457	5	11	4	F_1	2229.0416	0			14	2	A_2	2446.2466	−2		
7	3	F_2	2017.2789	−2			11	5	F_1	2232.7958	−1			14	3	A_2	2451.9980	−2		

7	4	F_2	2018.3647	−1			11	6	F_1	2233.2876	−3			14	1	E	2434.1330	−2
8	1	A_1	2059.3867	1			11	1	F_2	2223.7604	1			14	2	E	2435.7375	−1
8	2	A_1	2063.5885	−1			11	2	F_2	2226.6436	1	2059.8510	1	14	3	E	2441.6856	−7
8	1	A_2	2059.2363	−1	1848.4512	0	11	3	F_2	2229.0251	0			14	4	E	2446.2611	3
8	2	A_2	2060.9941	0	1881.4000	−4	11	4	F_2	2229.4411	0			14	5	E	2451.7632	−2
8	1	E	2060.5145	2			11	5	F_2	2232.8264	0			14	6	E	2454.1974	0
8	2	E	2061.9548	0	1881.5727	1	11	6	F_2	2233.2122	−2			14	1	F_1	2434.1047	1
8	3	E	2063.6111	−1			12	1	A_1	2288.1367	−1			14	2	F_1	2435.3121	−1
8	1	F_1	2059.3576	0			12	2	A_1	2300.2562	−1			14	3	F_1	2436.5455	3
8	2	F_1	2061.7396	−1			12	1	A_2	2287.2307	2	2129.7944	3	14	4	F_1	2441.6857	−4
8	3	F_1	2061.9603	1			12	2	A_2	2292.8977	−2			14	5	F_1	2444.3275	0
8	4	F_1	2063.6020	−1			12	3	A_2	2295.8489	2			14	6	F_1	2446.0680	4
8	1	F_2	2059.3065	0	1848.4341	1	12	1	E	2289.3025	−1			14	7	F_1	2446.4032	0
14	8	F_1	2452.8237	0			15	7	F_1	2529.4829	2			16	7	F_2	2618.3617	−4
14	9	F_1	2454.1148	1			15	8	F_1	2535.6847	−1			16	9	F_2	2627.8562	2
14	1	F_2	2435.8267	−1			15	9	F_1	2537.6262	0			16	10	F_2	2629.8022	0
14	2	F_2	2436.4915	2			15	10	F_1	2539.2737	−1			17	3	A_1	2722.5333	5
14	3	F_2	2444.3128	0			15	2	F_2	2517.6394	0			17	2	A_2	2697.5321	2
14	4	F_2	2446.2533	2			15	5	F_2	2529.5368	−1			17	4	A_2	2723.8672	−2
14	5	F_2	2451.8192	−3			15	6	F_2	2529.6567	5			17	5	E	2721.6326	0
14	6	F_2	2452.6143	1			15	7	F_2	2535.8068	−3			17	6	E	2726.0965	3
14	7	F_2	2454.2759	−1			15	8	F_2	2537.0161	2			17	7	F_1	2712.5016	2
15	1	A_1			2362.7110	3	15	9	F_2	2539.1115	2			17	9	F_1	2721.8161	1
15	2	A_1	2527.2918	0			16	1	A_1	2604.6622	2			17	11	F_1	2726.1646	−1
15	3	A_1	2529.3911	−1			16	3	A_1	2624.9583	−1			17	5	F_2	2705.2085	3
15	1	A_2	2517.8219	0			16	4	A_1	2629.9452	0			17	10	F_2	2723.5843	2
15	2	A_2	2536.6356	−1			16	3	A_2	2618.3945	0			17	11	F_2	2726.0248	0
15	1	E	2516.8578	2			16	4	A_2	2629.7128	1			18	1	E	2723.6304	0
15	2	E	2518.1374	1			16	2	E	2604.6331	−8			18	1	F_1	2724.0940	4
15	3	E	2527.2843	−2	2362.8211	3	16	3	E	2605.1511	−1			18	10	F_1	2822.5859	1
15	4	E	2529.6437	2			16	5	E	2618.2705	1			18	1	F_2	2723.3329	1
15	5	E	2537.2244	2			16	7	E	2627.6687	2			18	7	F_2	2810.3245	4
15	1	F_1	2515.6742	0			16	2	F_1	2604.6433	3			18	10	F_2	2822.2158	−1
15	2	F_1	2516.8896	0			16	4	F_1	2615.6528	−3			18	11	F_2	2825.1865	1
15	3	F_1	2517.5317	1	2362.7854	3	16	8	F_1	2627.0556	2			19	1	A_1	2828.4882	2
15	4	F_1	2518.1975	−1			16	9	F_1	2629.8786	3			19	1	A_2	2827.4497	−2
15	5	F_1	2524.1670	0			16	4	F_2	2605.1706	0			19	1	F_1	2828.0621	0
15	6	F_1	2527.2870	1			16	6	F_2	2615.6471	−4			19	1	F_2	2827.7310	−1

[a] In Table 4, δ is the difference $E^{exp.} - E^{calc.}$ in units of 10^{-4} cm^{-1}.

Table 5
Ro-vibrational term values for the $(0101, F_1)$ vibrational state of the $^{76}GeH_4$ molecule (in cm^{-1}).[a]

J	n	γ	$E(0101,F_1)$	δ	J	n	γ	$E(0101,F_1)$	δ	J	n	γ	$E(0101,F_1)$	δ	J	n	γ	$E(0101,F_1)$	δ	J	n	γ	$E(0101,F_1)$	δ
1	2	3	1	2	3	4	5	6	7	8	9	10	11	12	13	14	15	16	17	18	19	20	21	22
1	1	A_1	1760.9745	−1	7	2	A_2	1923.1628	−1	10	1	A_1	2047.2955	−2	12	2	E	2167.3796	1	14	3	A_2	2311.4458	1
1	1	E	1759.3600	3	7	3	A_2	1923.6438	1	10	2	A_1	2075.6747	−1	12	3	E	2169.9864	3	14	4	A_2	2326.4209	1
1	1	F_1	1760.1743	3	7	1	E	1902.0437	1	10	1	A_2	2014.1049	0	12	4	E	2177.0124	1	14	2	E	2311.0430	4
1	1	F_2	1758.6714	1	7	2	E	1921.0438	1	10	2	A_2	2044.9733	−1	12	5	E	2203.4049	−1	14	3	E	2314.6848	−1
3	1	A_1	1771.0112	2	7	3	E	1923.6163	0	10	3	A_2	2075.1793	−1	12	6	E	2205.2557	−3	14	4	E	2322.9050	4
2	2	A_2	1765.7970	−1	7	1	F_1	1877.7243	0	10	1	E	2013.8944	2	12	1	F_1	2131.6376	0	14	6	E	2355.8893	7
3	1	A_2	1792.2398	0	7	2	F_1	1899.8393	−1	10	2	E	2043.8967	−1	12	2	F_1	2132.0544	1	14	1	F_1	2269.9700	−1
2	1	E	1772.9210	−2	7	3	F_1	1901.0091	0	10	3	E	2046.2214	−1	12	3	F_1	2132.2779	−2	14	2	F_1	2270.8760	0
3	1	E	1793.2811	3	7	4	F_1	1920.8717	2	10	4	E	2050.5503	−1	12	4	F_1	2167.1769	2	14	4	F_1	2271.5923	0
2	1	F_1	1772.7084	0	7	5	F_1	1922.5100	0	10	5	E	2076.5364	0	12	5	F_1	2169.7872	2	14	5	F_1	2317.4192	−3
2	2	F_1	1774.2988	5	7	1	F_2	1877.4022	−1	10	1	F_1	2013.9176	0	12	6	F_1	2171.3573	−2	14	6	F_1	2320.2678	0
3	1	F_1	1780.8104	1	7	2	F_2	1900.0223	1	10	2	F_1	2014.3442	0	12	7	F_1	2174.0765	0	14	7	F_1	2323.1503	1
3	2	F_1	1791.8426	3	7	3	F_2	1900.8344	−1	10	3	F_1	2046.9929	0	12	8	F_1	2177.5485	2	14	8	F_1	2325.5978	1
2	1	F_2	1764.7764	−9	7	4	F_2	1902.2424	−1	10	4	F_1	2048.9526	−1	12	9	F_1	2203.3469	−1	14	11	F_1	2355.8059	6
3	1	F_2	1781.8796	1	7	5	F_2	1922.6944	−1	10	5	F_1	2050.8334	−2	12	10	F_1	2204.6736	−1	14	12	F_1	2357.8382	1
2	2	F_2	1773.3360	1	7	6	F_2	1923.5381	3	10	6	F_1	2075.4395	−2	12	11	F_1	2207.1403	−2	14	1	F_2	2271.2914	−1
3	2	F_2	1791.9718	0	8	1	A_1	1944.0055	−1	10	7	F_1	2076.3820	−3	12	1	F_2	2131.7606	3	14	3	F_2	2271.7136	6
3	3	F_2	1793.1823	2	8	1	A_2	1946.4234	0	10	8	F_1	2077.6997	0	12	2	F_2	2132.1841	−2	14	4	F_2	2311.1667	0
4	1	A_1	1802.6291	1	8	2	A_2	1968.7976	0	10	1	F_2	2013.8601	−1	12	3	F_2	2174.0800	−3	14	5	F_2	2314.9581	−1
4	1	A_2	1817.2569	1	8	1	E	1917.5237	2	10	2	F_2	2014.2488	−3	12	4	F_2	2176.5378	2	14	6	F_2	2320.0414	−8
4	1	E	1803.4740	0	8	2	E	1943.0563	−1	10	3	F_2	2044.1810	3	12	5	F_2	2203.5310	−3	14	7	F_2	2326.0625	2
4	2	E	1816.2714	−1	8	3	E	1944.3302	1	10	4	F_2	2045.8556	0	12	6	F_2	2205.4641	3	14	10	F_2	2357.8316	−2
4	1	F_1	1789.5640	−2	8	4	E	1966.4379	0	10	5	F_2	2047.1744	1	12	7	F_2	2207.1241	−3	15	1	A_1	2348.4724	−7
4	2	F_1	1802.3003	1	8	5	E	1968.3291	−1	10	6	F_2	2049.6195	1	13	1	A_1	2199.0834	2	15	2	A_1	2349.2822	5
4	3	F_1	1803.5402	2	8	1	F_1	1917.5296	−1	10	7	F_2	2075.2994	−4	13	2	A_1	2241.1689	−2	15	3	A_1	2406.0566	0
4	4	F_1	1816.3295	0	8	2	F_1	1917.8930	0	10	8	F_2	2077.6080	−3	13	3	A_1	2244.6163	1	15	1	A_2	2400.9342	−6
4	5	F_1	1817.7411	2	8	3	F_1	1943.0227	−2	11	1	A_1	2070.6631	−2	13	4	A_1	2275.1660	4	15	2	A_2	2441.0980	2
4	1	F_2	1816.2742	1	8	4	F_1	1944.1897	0	11	2	A_1	2111.6013	1	13	5	A_1	2279.8465	−3	15	3	F_1	2348.9158	2
4	2	F_2	1817.5632	1	8	5	F_1	1945.6767	0	11	3	A_1	2137.7097	0	13	1	A_2	2199.0849	−4	15	5	F_1	2390.9634	6
5	1	A_1	1831.0204	1	8	6	F_1	1968.0604	−1	11	1	A_2	2109.4932	1	13	2	A_2	2275.3614	0	15	6	F_1	2395.0596	−4
5	2	A_1	1847.7108	1	8	7	F_1	1969.6521	0	11	2	A_2	2139.6856	−1	13	1	E	2197.8780	−1	15	7	F_1	2404.9439	0
5	1	E	1813.5592	1	8	1	F_2	1917.6703	−2	11	1	E	2070.1098	−2	13	2	E	2198.7667	1	15	3	F_2	2355.7772	−8
5	2	E	1845.8950	1	8	2	F_2	1943.8819	2	11	2	E	2070.5372	1	13	3	E	2199.3000	−2	15	4	F_2	2391.1317	2
5	3	E	1847.4648	2	8	3	F_2	1946.0743	−2	11	3	E	2106.4514	−1	13	4	E	2244.3772	1	15	5	F_2	2398.6663	1
5	1	F_1	1829.6217	0	8	4	F_2	1966.2758	−3	11	4	E	2108.8611	−2	13	5	E	2248.7991	1	15	6	F_2	2401.1007	−2
5	2	F_1	1830.7130	0	8	5	F_2	1968.4593	1	11	5	E	2136.8199	−2	13	6	E	2276.9970	7	15	7	F_2	2404.4881	2
5	3	F_1	1845.8468	3	8	6	F_2	1969.4025	−1	11	6	E	2139.7473	−3	13	1	F_1	2198.5013	−2	16	2	A_1	2476.0378	2
5	4	F_1	1847.5695	1	9	1	A_1	1963.0322	−2	11	1	F_1	2070.0375	−1	13	2	F_1	2199.0699	2	16	2	E	2476.2078	4
5	1	F_2	1813.4892	1	9	2	A_1	1994.3255	−1	11	2	F_1	2070.5880	−3	13	3	F_1	2236.3471	3	16	1	F_1	2431.3168	−1
5	2	F_2	1830.4816	−1	9	3	A_1	2021.0919	0	11	3	F_1	2102.8557	0	13	4	F_1	2239.7144	1	16	2	F_1	2431.8876	5
5	3	F_2	1846.0957	−1	9	1	A_2	1963.1178	−1	11	4	F_1	2105.3869	1	13	5	F_1	2242.0150	2	16	7	F_1	2493.5231	9
5	4	F_2	1847.0019	2	9	2	A_2	2016.8213	−2	11	5	F_1	2111.2333	−1	13	6	F_1	2244.4961	1	16	3	F_2	2487.3068	−2
6	1	A_1	1880.6768	1	9	1	E	1963.4357	−1	11	6	F_1	2136.9071	−1	13	7	F_1	2248.0182	1	17	4	F_1	2571.5218	−7
6	1	A_2	1842.6742	0	9	2	E	1992.6090	0	11	7	F_1	2138.1054	0	13	8	F_1	2275.2275	3	17	1	F_2	2519.5142	2
6	2	A_2	1862.7555	0	9	3	E	1995.2393	0	11	1	F_2	2070.1796	2	13	9	F_1	2277.7828	4	18	4	F_2	2667.5818	−3
6	1	E	1861.9632	0	9	4	E	2019.1279	−1	11	2	F_2	2070.3971	1	13	10	F_1	2279.8364	−3					
6	2	E	1863.2030	2	9	5	E	2020.8356	−1	11	3	F_2	2103.2466	−3	13	1	F_2	2197.9027	2					
6	3	E	1882.1760	1	9	1	F_1	1963.0282	1	11	4	F_2	2105.0585	−1	13	2	F_2	2198.7818	4					

6	1	F_1	1842.9482	1	9	2	F_1	1992.2899	0	11	5	F_2	2106.7951	0	13	3	F_2	2199.0623	−1
6	2	F_1	1863.8454	−4	9	3	F_1	1992.8919	−1	11	6	F_2	2108.9342	−1	13	4	F_2	2199.2576	0
6	3	F_1	1880.7774	0	9	4	F_1	1994.8702	−1	11	7	F_2	2110.7662	1	13	5	F_2	2236.7394	3
6	4	F_1	1882.0687	1	9	5	F_1	2019.4451	0	11	8	F_2	2136.6745	−1	13	6	F_2	2239.9064	2
6	5	F_1	1882.9470	1	9	6	F_1	2020.9040	0	11	9	F_2	2138.4076	0	13	7	F_2	2246.6098	0
6	1	F_2	1842.8434	0	9	1	F_2	1963.0367	1	11	10	F_2	2139.7402	−2	13	8	F_2	2249.1256	1
6	2	F_2	1862.2051	−1	9	2	F_2	1963.3735	−2	12	1	A_1	2131.5262	−3	13	9	F_2	2275.2917	2
6	3	F_2	1863.0373	0	9	3	F_2	1991.3793	−1	12	2	A_1	2166.7418	0	13	10	F_2	2276.7975	5
6	4	F_2	1880.9359	−2	9	4	F_2	1993.1578	0	12	3	A_1	2169.7896	−1	13	11	F_2	2278.1269	2
6	5	F_2	1882.7237	0	9	5	F_2	1995.8231	−2	12	1	A_2	2131.8938	3	14	1	A_1	2269.9457	−1
7	1	A_1	1877.7662	0	9	6	F_2	2016.9803	−1	12	2	A_2	2175.5192	−1	14	2	A_1	2324.7166	1
7	2	A_1	1922.3279	−1	9	7	F_2	2019.0355	−3	12	3	A_2	2205.7632	3	14	3	A_1	2355.5054	4
7	1	A_2	1900.4679	2	9	8	F_2	2019.9685	−2	12	1	E	2132.0740	5	14	1	A_2	2270.7886	−5

[a] In Table 5, δ is the difference $E^{exp.}-E^{calc.}$ in units of 10^{-4} cm^{-1}.

vibrational states ($v\Gamma$) and ($v'\Gamma'$) for which the relation (see, e.g., [36])

$$\Gamma \otimes \Gamma' \in F_2 \quad (1)$$

is fulfilled (the $\otimes$ denotes a tensorial product). So, from the ground vibrational state (symmetry is A_1) transitions are allowed by symmetry only to the F_2-type vibrational states (in our case, they are the $\nu_2+\nu_4(F_2)$ and $2\nu_4(F_2)$ sub-bands). Transitions to the vibrational states of any other symmetry can appear in the absorption spectra only because of resonance interactions with the F_2-type vibrational states (in our case, they are the $2\nu_4(E)$, $2\nu_4(A_1)$, $\nu_2+\nu_4(F_1)$, $2\nu_2(A_1)$ and $2\nu_2(E)$ sub-bands). In this case, because the resonance interactions are strong, a picture of even the $\nu_2+\nu_4(F_2)$ and $2\nu_4(F_2)$ bands is far from the regular J-cluster structure which is typical for the F_2-type bands.

At the first step of analysis of the $^{76}GeH_4$ isotopologue, the Ground State Combination Differences method (see, e.g., Refs. [37–39]) was used. In this case, energy values of the ground vibrational state were calculated with the parameters from Ref. [32]. As the result of assignment, about 450, 300, 40, 10, 80 and 340 transitions were assigned to the $\nu_2+\nu_4(F_2)$, $\nu_2+\nu_4(F_1)$, $2\nu_4(F_2)$, $2\nu_4(E)$, $2\nu_2(A_1)$ and $2\nu_2(E)$ sub-bands of $^{76}GeH_4$, respectively. The second step of assignment was made after fit of the transitions assigned at the first step. Finally, about 800, 700, 100, 30, 130 and 500 transitions with the maximum value of upper quantum number $J^{max.}$ equal to 19, 18, 15, 13, 18 and 19 were assigned to the six mentioned ro-vibrational bands, respectively (see also the statistical information in Table 2). A complete list of assigned transitions is presented in the Supplementary I. The obtained results were used then for determination of the energy values of the upper ro-vibrational states.

As the third step, the "hot" experimental Dyad–Pentad transitions from the region of 700–1080 cm^{-1} were additionally assigned which essentially enriched information about the upper ro-vibrational energies. Transitions from this region were assigned to the eight "hot" sub-bands: $\nu_2+\nu_4(F_2)-\nu_2$ (236 transitions), $\nu_2+\nu_4(F_1)-\nu_2$ (179 transitions), $2\nu_2(E)-\nu_2$ (81 transitions), $\nu_2+\nu_4(F_2)-\nu_4$ (119 transitions), $\nu_2+\nu_4(F_1)-\nu_4$ (45 transitions), $2\nu_4(F_2)-\nu_4$ (206 transitions) and $2\nu_4(E)-\nu_4$ (52 transitions). Additionally we assigned without doubt (validity of assignment was confirmed by the values of the relative line strengths and by presence of ground state combination differences) 76 transitions (29 upper energies) belonging to the "hot" $2\nu_4(A_1)-\nu_4$ sub-band (for more details, see statistical information in Table 2). A complete list of the "hot" assigned transitions is presented in the Supplementary II.

Analogous to $^{76}GeH_4$, the transitions of the $^{74}GeH_4$ isotopologue were assigned both in the "cold" (1450–2000 cm^{-1}) and in the "hot" (700–1080 cm^{-1}) ro-vibrational bands. Results of assignment are added to the Supplementary Materials I and II, and corresponding statistical information can be found in Table 2.

4. Theoretical background and the hamiltonian model

High symmetry of the molecule leads to necessity of using the special mathematical formalism (theory of

Irreducible Tensorial Sets, see, e.g., [40–42] and the recent review in Ref. [43]) for description of its spectra. Different aspects of application of that formalism to the XY_4 (T_d–symmetry) molecules were discussed in the spectroscopic literature many times (we do not reproduce here a very long list of the corresponding papers and refer the reader to the classical papers by Hecht, Ref. [44], Moret-Bailly, Ref. [45], and Champion, Ref. [46], on the one hand, and to recent review of Boudon, et al., Ref. [47], on the other hand). For that reason, only a brief theoretical basis of our present study is given in this section.

(*a*) *Irreducible rotational operators of the SO(3) group*: In accordance with general statements of the Irreducible Tensorial Sets Theory [40–42], the basic first-rank irreducible rotational operators $R_m^{\Omega(K)}$ ($m=0, \pm 1, \ldots, \pm K$) can be chosen in the following form[2]:

$$R_1^{1(1)} = -\frac{1}{\sqrt{2}}\left(J_x - iJ_y\right) \equiv -J_+,$$
$$R_{-1}^{1(1)} = \frac{1}{\sqrt{2}}\left(J_x + iJ_y\right) \equiv J_-,$$
$$R_0^{1(1)} = J_z \equiv J_0. \tag{2}$$

In operators $R_m^{\Omega(K)}$ the following notations are used: Ω is the total degree of rotational operators J_α, $\alpha = x,y,z$ (for example, for $\Omega=1$, $R_{\ldots}^{1(\ldots)} \sim J_\alpha$; for $\Omega=2$, $R_{\ldots}^{2(\ldots)} \sim J_\alpha J_\beta$; etc.); the indexes K and m indicate the irreducible representation $D^{(K)}$ of the $SO(3)$ symmetry group and its line, in accordance with those the operators $R_m^{\Omega(K)}$ are transformed under operations from $SO(3)$; the operators J_α are conventional angular momentum components related to the molecular fixed coordinate system:

$$J_x = i\frac{\cos\varphi}{\sin\theta}\left(\frac{\partial}{\partial\psi} - \cos\theta\frac{\partial}{\partial\varphi}\right) - i\sin\varphi\frac{\partial}{\partial\theta},$$
$$J_y = -i\frac{\sin\varphi}{\sin\theta}\left(\frac{\partial}{\partial\psi} - \cos\theta\frac{\partial}{\partial\varphi}\right) - i\cos\varphi\frac{\partial}{\partial\theta}, \tag{3}$$

and

$$J_z = -i\frac{\partial}{\partial\varphi}. \tag{4}$$

Irreducible rotational operators $R_{\tilde{m}}^{\Omega+1(K+1)}$ can be constructed from corresponding irreducible rotational operators $R_m^{\Omega(K)}$ ($n=0, \pm 1, \ldots \pm K$) and $R_l^{1(1)}$ ($l=0, \pm 1$) of lower degrees and ranks in accordance with the general rule [48,49],

$$R_{\tilde{m}}^{\Omega+1(K+1)} = \sum_{l=-1,0,1} C_{K\tilde{m}-l,1l}^{K+1\tilde{m}} R_{\tilde{m}-l}^{\Omega(K)} R_l^{1(1)}, \tag{5}$$

where $C_{K\tilde{m}-l,1l}^{K+1\tilde{m}}$ are known Clebsh–Gordan coefficients, Ref. [42]. Irreducible rotational operators $R_m^{\Omega(K)}$ with $K<\Omega$ (in this case, the parity of both Ω, and K must be the same) are constructed as,

$$R_m^{\Omega(K)} = R_m^{\Omega=K(K)}\left(R^{2(0)}\right)^{(\Omega-K)/2}, \tag{6}$$

where we use the notation $R^{2(0)} = (J_x^2 + J_y^2 + J_z^2)$.

[2] We would like to mark that the definition of the basic $R_m^{1(1)}$ ($m=0, \pm 1$) operators in Eq. (2) differs in coefficients from the definition of corresponding $R_m^{1(1)}$ ($m=0, \pm 1$) operators in Refs. [45,46]. However this fact does not break the general properties and equivalence of obtained results.

(*b*) *Irreducible rotational operators of the T_d group*: Different rotational operators $R_\sigma^{\Omega(K,n\Gamma)}$, that are symmetries in accordance with irreducible representations $\Gamma = A_1, A_2, E, F_1$, or F_2 of the T_d symmetry group, can be easily constructed from the above discussed operators $R_m^{\Omega(K)}$ by using the following general relations [43],

$$R_\sigma^{\Omega(K,n\Gamma)} = \sum_m {}^{(K)}G_{n\Gamma\sigma}^m R_m^{\Omega(K)}. \tag{7}$$

The reduction matrix elements ${}^{(K)}G_{n\Gamma\sigma}^m$, which are presented in Eq. (7), are determined by the concrete point symmetry group. Speaking about molecules of the T_d symmetry, only the numerical representation of the ${}^{(K)}G_{n\Gamma\sigma}^m$ values was used (see, e.g., [50,51]). In our case, we used considerably more convenient analytical representation of G-matrix elements, see, e.g., [52,53].

(*c*) *Ro-vibrational functions in the symmetrized form*: The T_d symmetry group has five irreducible representations A_1, A_2, E (E_1 or E_2), F_1 (F_{1x}, F_{1y}, F_{1z}) and F_2 (F_{2x}, F_{2y}, F_{2z}). For that reason, any of vibration–rotation wave functions should be totally symmetric (A_1), antisymmetric (A_2), or be transformed under symmetry operations according to one from two (E_1 or E_2), or three (F_{1x}, F_{1y}, F_{1z}), (F_{2x}, F_{2y}, F_{2z}) lines of irreducible representations E, F_1, F_2. In general case, any vibration–rotation function can be constructed in the following form [54,55]:

$$|v\gamma_v; Jn_J\gamma_r; m\gamma s\rangle \equiv \left(|v\gamma_v\rangle \otimes |Jn_J\gamma_r\rangle\right)_s^\gamma$$
$$= \sqrt{[\gamma]}\sum_{\sigma_v\sigma_r}\begin{pmatrix}\gamma & \gamma_v & \gamma_r\\ s & \sigma_v & \sigma_r\end{pmatrix}|v\gamma_v\sigma_v\rangle|Jn_J\gamma_r\sigma_r\rangle, \tag{8}$$

where the set of indices $v\gamma_v$, $Jn_J\gamma_r$, and $m\gamma s$ unambiguously determines any symmetrized vibration–rotation function, and the indices γ_v, γ_r, and γ are the symmetry of vibrational, rotational, and vibrational–rotational functions, respectively. The $|v\gamma_v\sigma_v\rangle$ and $|Jn_J\gamma_r\sigma_r\rangle$ in Eq. (8) are pure vibrational and rotational wave functions (in our case, symmetrized in the T_d group); the symbols $\otimes$ and $[\gamma]$ denote a direct tensorial product and dimension of the irreducible representation γ, respectively; the values $\begin{pmatrix}\gamma & \gamma_v & \gamma_r\\ s & \sigma_v & \sigma_r\end{pmatrix}$ are the 3Γ-symbols of the symmetry group.

The pure rotational functions, $|Jn_J\gamma_r\sigma_r\rangle$, being the functions, in our case, symmetrized in the T_d symmetry group, can be constructed in accordance with the general equation analogous to Eq. (8):

$$|Jn_J\gamma_r\sigma_r\rangle = \sum_k {}^{(J)}G_{n_J\gamma_r\sigma_r}^k |Jk\rangle. \tag{9}$$

The coefficients ${}^{(J)}G_{n_J\gamma_r\sigma_r}^k$ in analytical form can be found, e.g., in Ref. [52]; the $|Jk\rangle$ ($-J \le k \le J$) are the conventional rotational functions, see, e.g., Ref. [56].

(*d*) *Effective Hamiltonian*: It is well known, Refs. [57], that the most efficient way of describing ro-vibrational structure of polyatomic molecules is the use of so-called effective Hamiltonians. In general case, the effective Hamiltonian can be presented in the following form:

$$H^{vib.-rot.} = \sum_{a,b}|a\rangle\langle b|H^{a,b}. \tag{10}$$

Here $|a\rangle$ and $\langle b|$ are the basic vibrational functions; operators $H^{a,b}$ depend on rotational operators, J_α, only; and

Table 6
Ro-vibrational term values for the $(0101, F_2)$ and $(0002, F_2)$ vibrational states of the $^{76}GeH_4$ molecule (in cm^{-1}).[a]

J	n	γ	$E(0101, F_2)$	δ	$E(0002, F_2)$	δ	J	n	γ	$E(0101, F_2)$	δ	$E(0002, F_2)$	δ	J	n	γ	$E(0101, F_2)$	δ	$E(0002, F_2)$	δ
1			2	3	4	5	1			2	3	4	5	1			2	3	4	5
0	1	F_2	1748.3964	1			6	5	F_1	1884.5837	1			9	4	A_2			1931.1614	0
1	1	A_2	1757.5299	3	1650.0144	−3	6	1	F_2	1842.0314	−1	1709.8146	2	9	1	E	1962.2701	1	1819.1866	−5
1	1	E	1749.1642	−3			6	2	F_2	1842.5434	−2	1724.3121	−0	9	2	E	1964.7678	−1	1841.0512	−2
1	1	F_1	1751.1870	1	1636.6950	0	6	3	F_2	1860.0265	2			9	3	E	1989.2357	1		
1	1	F_2	1753.3088	4	1643.1853	2	6	4	F_2	1882.8983	1	1762.3137	2	9	4	E	2021.8825	−5	1897.2200	−0
1	2	F_2			1651.5837	−0	6	5	F_2			1763.4358	1	9	5	E	2026.4146	0	1924.7604	1
2	1	A_1	1760.9589	−3	1638.4281	−0	7	1	A_1	1899.6254	1	1802.1330	3	9	1	F_1	1962.1956	1	1818.9423	−3
2	1	E	1763.2480	−0	1668.3528	1	7	2	A_1	1926.3057	1	1827.4898	−6	9	2	F_1	1964.2131	−1	1820.6697	1
2	1	F_1	1757.1867	0	1641.3922	0	7	1	A_2	1877.8264	−1			9	3	F_1	1964.7521	−1	1841.0072	1
2	2	F_1	1762.3379	−0	1655.5567	1	7	2	A_2			1779.8069	4	9	4	F_1	1984.3661	−1		
2	1	F_2	1756.7948	1	1646.9861	−0	7	3	A_2			1825.2658	−0	9	5	F_1	1990.2329	2	1869.8142	0
2	2	F_2	1772.4840	−0	1656.4469	1	7	1	E	1876.7404	−1			9	6	F_1	2017.1666	−0		
3	1	A_1	1792.0516	−2	1674.2540	0	7	2	E	1877.5521	2	1757.7341	3	9	7	F_1	2021.5973	−0		
3	1	A_2	1769.8362	2			7	3	E	1877.7954	−2			9	8	F_1	2023.7106	3	1898.8897	−8
3	1	E	1770.1445	−1	1654.1166	2	7	4	E	1897.6319	1	1802.0423	−1	9	9	F_1			1924.3691	3
3	2	E	1780.3420	−1	1674.8223	1	7	5	E	1926.5678	−2			9	10	F_1			1928.0025	0
3	3	E	1792.3670	−1	1688.9887	2	7	1	F_1	1876.6912	−1	1740.9115	−2	9	1	F_2	1962.3383	−0	1819.3550	−2
3	1	F_1	1770.4725	−0	1648.3936	−0	7	2	F_1	1877.4252	0	1741.8220	−3	9	2	F_2	1964.1701	1	1820.5418	−2
3	2	F_1	1777.4916	−3	1674.5960	2	7	3	F_1	1894.3820	−1			9	3	F_2	1984.4655	−1		
3	3	F_1	1792.2911	2	1688.6230	1	7	4	F_1	1897.9063	2	1802.0697	0	9	4	F_2	1988.9120	2		
3	1	F_2	1769.9646	−1	1654.4591	1	7	5	F_1	1924.4201	2			9	5	F_2	2023.0418	−0	1897.2173	−1
3	2	F_2	1778.7691	2	1663.1224	1	7	6	F_1	1926.4939	0	1826.2778	−3	9	6	F_2	2026.4583	−1		
4	1	A_1	1816.8091	2	1714.9138	1	7	7	F_1			1828.9231	−2	9	7	F_2			1925.6000	0
4	1	A_2	1800.2230	0	1717.7400	2	7	1	F_2	1876.7829	−2	1741.5720	−1	9	8	F_2			1930.6587	2
4	1	E	1788.7501	0	1663.7141	1	7	2	F_2	1877.7817	1	1757.8373	−0	10	1	A_1	2015.8379	1	1868.1917	1
4	2	E	1798.8352	1			7	3	F_2	1894.6252	−2			10	2	A_1	2037.1959	−3		
4	1	F_1	1788.6137	−3	1672.1616	1	7	4	F_2	1921.2470	1			10	3	A_1	2078.1648	2		
4	2	F_1	1817.4650	3	1698.5150	−1	7	5	F_2	1924.0135	9	1803.2530	−1	10	1	A_2	2047.4995	1		
4	3	F_1			1715.4268	−0	7	6	F_2			1825.7147	−2	10	2	A_2	2080.5602	−1	1982.9658	1
4	1	F_2	1788.5847	−3	1663.6264	1	8	1	A_1	1916.7217	1	1777.2013	−0	10	1	E	2013.0728	−1	1866.0629	−2
4	2	F_2	1788.9175	1	1672.6804	−1	8	2	A_1	1941.6971	2			10	2	E	2015.7368	−2	1868.0488	−1
4	3	F_2	1799.1173	−1			8	3	A_1	1971.5774	2	1875.3022	−2	10	3	E	2037.2887	−2		
4	4	F_2	1801.7781	1			8	1	A_2	1916.9233	1	1778.2468	−3	10	4	E	2072.8921	1		
4	5	F_2	1817.6919	2	1715.9959	−3	8	2	A_2	1936.9960	−0			10	5	E	2081.4191	1		
5	1	A_1	1812.6500	2	1695.2367	1	8	1	E	1918.1228	0	1778.5606	−1	10	1	F_1	2013.1530	1	1866.4165	−1
5	1	A_2	1812.8315	0	1683.9873	−2	8	2	E	1936.7511	−1			10	2	F_1	2015.7781	−2	1868.1019	2
5	2	A_2	1827.6029	−1	1727.8454	4	8	3	E	1970.7409	−0			10	3	F_1	2016.4548	−1	1890.4169	−3
5	3	A_2	1848.5961	2			8	5	E			1872.9941	−1	10	4	F_1	2037.2572	1		
5	1	E	1812.8154	−2	1695.8983	−1	8	1	F_1	1916.7833	1	1777.3603	−2	10	5	F_1	2042.5921	−1	1922.6166	5
5	2	E	1829.3115	3			8	2	F_1	1918.4950	0	1796.7393	1	10	6	F_1	2073.0701	1		
5	3	E	1848.2617	−1	1727.8360	3	8	3	F_1	1941.0387	2			10	7	F_1	2078.6701	2		
5	4	E			1747.5453	2	8	4	F_1	1966.6682	−2	1847.0502	2	10	8	F_1	2084.5679	−1		
5	1	F_1	1812.6675	−1	1684.3725	−1	8	5	F_1	1971.0748	−0			10	9	F_1			1981.5556	3
5	2	F_1	1812.7990	−1	1695.6295	4	8	6	F_1	1973.6900	0	1848.5710	3	10	1	F_2	2013.0216	1	1865.9549	−4
5	3	F_1	1825.4343	2			8	7	F_1			1873.5526	0	10	2	F_2	2015.6196	−1	1866.8611	−2
5	4	F_1	1847.1642	−1	1746.7935	2	8	8	F_1			1876.8150	−1	10	3	F_2	2016.4716	1	1890.4687	1
5	1	F_2	1812.7221	−1	1684.1944	−1	8	1	F_2	1916.8505	2	1777.5466	−4	10	4	F_2	2042.0735	2		
5	2	F_2	1825.8721	−0			8	2	F_2	1918.1479	0	1778.4835	−2	10	5	F_2	2072.7230	1		

Table 6 (*continued*)

J	n	γ	$E(0101,F_2)$	δ	$E(0002,F_2)$	δ	J	n	γ	$E(0101,F_2)$	δ	$E(0002,F_2)$	δ	J	n	γ	$E(0101,F_2)$	δ	$E(0002,F_2)$	δ
1			2	3	4	5	1			2	3	4	5	1			2	3	4	5
5	3	F_2	1828.8480	1	1727.8390	5	8	3	F_2	1918.5418	−1	1796.8770	−0	10	6	F_2	2079.1660	2		
5	4	F_2	1848.3974	1	1748.0491	0	8	4	F_2	1936.8261	−3			10	7	F_2	2081.2237	−0		
6	5	F_2	1884.8026	1			8	5	F_2	1940.5436	1			10	8	F_2	2084.6265	−6		
6	1	A_1	1842.3748	1	1710.5100	−2	8	6	F_2	1969.9869	1			10	10	F_2			1985.6874	−1
6	2	A_1	1857.1357	−1			8	7	F_2	1973.8055	0	1847.0133	−2	10	11	F_2			1989.7236	−1
6	1	A_2	1881.2146	−0	1763.4320	1	8	8	F_2			1872.3729	1	11	1	A_1	2069.3512	−2	1918.8829	−1
6	1	E	1842.0155	1	1710.1781	−3	8	9	F_2			1877.4046	−1	11	2	A_1	2101.3674	3	1950.4795	−7
6	2	E	1857.6142	−2	1725.8893	3	9	1	A_1	1964.7175	−1	1840.9253	1	11	3	A_1	2148.1092	−2		
6	3	E	1883.0653	1			9	2	A_1	2017.3955	3			11	4	A_1			2053.1580	−2
6	1	F_1	1842.0438	−1	1710.3144	0	9	3	A_1			1899.0319	3	11	1	A_2	2069.1912	1	1918.1971	−3
6	2	F_1	1842.4840	−2	1723.9468	2	9	1	A_2	1964.1272	−0	1819.6847	−2	11	2	A_2	2073.6400	−2	1945.1400	−1
6	3	F_1	1857.4298	−1			9	2	A_2	1988.4401	1			11	3	A_2	2104.4018	−1		
6	4	F_1	1861.6286	2	1762.3633	1	9	3	A_2	2026.5376	−2	1897.2130	−2	11	4	A_2	2142.6285	0		
11	1	E	2072.6285	−1	1919.4557	−6	12	11	F_2	2210.6232	2	2115.2324	1	14	8	F_1	2359.7601	2		
11	2	E	2073.6326	−2	1945.0956	1	12	12	F_2	2217.1024	−3	2123.0925	−3	14	9	F_1	2362.5709	0		
11	3	E	2100.7964	3			13	1	A_1	2204.2936	−1	2070.1234	1	14	10	F_1	2371.0481	2		
11	4	E	2133.8782	−0			13	2	A_1	2282.4856	3			14	15	F_1			2277.7836	2
11	5	E	2141.2340	1			13	1	A_2	2203.1214	3	2040.7958	3	14	1	F_2	2269.8384	1	2107.2277	0
11	6	E	2148.1682	−4			13	2	A_2	2233.8279	1			14	2	F_2	2270.5614	−5	2108.1071	−1
11	8	E			2053.7679	1	13	3	A_2	2242.6553	−0			14	3	F_2	2276.1554	−3	2109.3649	4
11	1	F_1	2069.2855	−5	1918.4888	−2	13	4	A_2	2280.5266	−1			14	4	F_2	2276.4203	1	2140.4818	−5
11	2	F_1	2072.5991	1	1919.3424	−3	13	5	A_2	2291.4142	−0			14	5	F_2	2277.7286	2		
11	3	F_1	2072.8821	1	1920.9853	2	13	1	E	2203.0838	1			14	6	F_2	2308.2758	2		
11	4	F_1	2095.3306	−4			13	2	E	2204.2859	2	2040.5269	8	14	7	F_2	2313.9799	−2		
11	5	F_1	2100.9471	2			13	3	E	2234.0545	3			14	8	F_2	2318.3942	2		
11	6	F_1	2106.9710	−2			13	4	E	2238.9987	−2			14	10	F_2	2358.7129	2		
11	7	F_1	2133.7370	1	2013.2444	−4	13	5	E	2271.3694	−1			14	11	F_2	2363.1022	−4		
11	8	F_1	2140.5123	3	2014.2053	−3	13	6	E	2284.1741	−1			14	12	F_2	2366.3124	−3		
11	9	F_1	2144.5593	−3			13	7	E	2291.3909	−4			14	13	F_2	2371.0571	1	2266.7924	6
11	10	F_1	2148.1491	−3			13	9	E			2188.4943	6	14	14	F_2			2277.9237	5
11	11	F_1			2049.5233	−1	13	1	F_1	2197.6639	−2	2038.8121	0	15	1	A_1	2355.4467	1	2183.1584	8
11	12	F_1			2053.5935	−5	13	2	F_1	2202.9839	−1	2039.7589	−3	15	2	A_1	2387.9490	−1		
11	1	F_2	2069.2347	1	1918.3243	−0	13	3	F_1	2203.1974	−5	2042.6999	5	15	3	A_1	2429.5787	−1		
11	2	F_2	2072.8304	−1	1920.9132	1	13	4	F_1	2204.2887	2	2070.1320	−4	15	4	A_1	2456.0229	8		
11	3	F_2			1945.1102	1	13	5	F_1	2227.2617	−3			15	1	A_2	2348.2559	1		
11	4	F_2	2095.3685	−4			13	6	F_1	2239.1888	−1			15	2	A_2	2355.3070	−4	2216.0478	5
11	5	F_2	2134.0487	0			13	7	F_1	2271.2543	1			15	3	A_2	2356.5556	−4		
11	6	F_2	2141.6836	−1			13	8	F_1	2281.4769	1	2151.4075	−5	15	4	A_2	2393.9920	−2		
11	7	F_2	2144.2242	1			13	9	F_1	2283.8723	−1			15	5	A_2	2429.3269	−4		
11	11	F_2			2048.6740	−1	13	10	F_1	2287.0778	−3			15	6	A_2	2447.6713	−2		
12	1	A_1	2135.0289	−1	1976.6841	−2	13	11	F_1			2187.9096	1	15	1	E			2180.7108	6
12	2	A_1	2199.8558	2			13	12	F_1			2192.3200	−0	15	2	E	2355.1789	−3		
12	3	A_1	2213.2474	−1			13	1	F_2	2203.0935	−1	2039.1318	2	15	3	E	2356.5601	8		
12	4	A_1			2118.7580	−1	13	2	F_2	2203.2541	−2	2040.6310	1	15	4	E	2387.8652	−0		
12	1	A_2	2135.4212	−1			13	3	F_2	2227.2741	−2			15	5	E	2395.0206	−0		
12	2	A_2	2158.7103	−3			13	4	F_2	2233.9729	2			15	6	E	2442.3628	−0		
12	3	A_2	2200.2649	4			13	5	F_2	2242.4816	2			15	7	E	2446.9150	0		
12	1	E	2130.8400	2	1976.0397	0	13	6	F_2	2271.4873	3			15	10	E			2349.8540	5
12	2	E	2135.4400	3	1979.1711	−1	13	7	F_2	2280.9578	−1			15	2	F_1	2354.8802	2		

12	3	E	2158.6773	−1			13	8	F_2	2286.8578	−1			15	3	F_1	2355.2726	−3	2183.2804	7
12	4	E	2172.0415	−1			13	9	F_2	2291.3989	−1			15	4	F_1	2355.6420	−1		
12	5	E	2208.3671	3			13	13	F_2			2191.1900	−3	15	6	F_1	2387.8923	−1		
12	6	E	2212.8426	−1			14	1	A_1	2276.7141	1	2107.0051	3	15	7	F_1	2396.3462	−1		
12	8	E			2117.2439	1	14	2	A_1	2301.0761	−2			15	10	F_1	2442.0138	1		
12	1	F_1	2130.8462	3	1976.1948	−0	14	3	A_1	2315.5057	−3			15	11	F_1	2445.1783	−1		
12	2	F_1	2135.0794	−2	1977.2035	−1	14	4	A_1	2361.3858	−4			15	12	F_1	2451.0334	0		
12	3	F_1	2136.2515	4	2004.9995	−1	14	1	A_2	2269.1130	1	2107.4507	5	15	13	F_1	2456.0279	6		
12	4	F_1	2164.9645	2			14	2	A_2	2315.1480	1			15	15	F_1			2356.2078	0
12	5	F_1	2199.9801	−1			14	3	A_2	2366.1526	1			15	1	F_2	2347.1432	−1	2180.8278	3
12	6	F_1	2209.3254	2			14	1	E	2270.5601	−4	2108.2334	−0	15	2	F_2	2348.3156	−1		
12	7	F_1	2212.9970	−1			14	2	E	2276.4244	1			15	3	F_2	2354.9219	4		
12	8	F_1	2217.0774	−5			14	3	E	2276.8128	−3			15	4	F_2	2355.6710	2		
12	11	F_1			2117.8335	0	14	6	E	2347.8357	1			15	5	F_2	2356.5585	1		
12	12	F_1			2122.8172	−2	14	7	E	2359.2712	−1			15	6	F_2	2380.1281	5		
12	1	F_2	2130.7869	1	1975.8693	−5	14	8	E	2366.3829	−2			15	7	F_2	2394.5012	−2		
12	2	F_2	2135.1237	2	1977.4039	−1	14	9	E			2271.7172	6	15	8	F_2	2395.4025	2		
12	3	F_2	2135.4344	3	1979.1483	3	14	1	F_1	2276.2791	−2	2107.1017	0	15	9	F_2	2429.4076	−1		
12	4	F_2			2005.0164	3	14	2	F_1	2276.7852	−0	2109.2061	5	15	10	F_2	2443.0505	−1		
12	5	F_2	2158.6883	−1			14	3	F_1	2277.7337	1			15	11	F_2	2447.2143	−1		
12	6	F_2	2164.7401	1			14	4	F_1	2301.0825	−4	2140.4770	−3	15	12	F_2	2450.9384	1		
12	7	F_2	2169.1425	0			14	5	F_1	2308.3735	1			15	13	F_2			2350.5197	−1
12	8	F_2	2172.0126	−3			14	6	F_1	2314.6778	−0			16	1	A_1	2439.3198	3		
12	10	F_2	2208.0244	3			14	7	F_1	2347.9389	−1			16	3	A_1	2530.3554	2		
16	4	A_1	2541.0315	2			16	13	F_2	2531.1554	3			17	3	F_2	2529.0380	1		
16	1	A_2	2439.9480	2			16	14	F_2	2534.1316	−4			17	4	F_2	2529.5460	2		
16	4	A_2	2531.8207	1			16	15	F_2	2537.1281	0			17	5	F_2	2529.6319	1		
16	1	E	2430.0682	6			16	16	F_2	2546.3008	−2			17	11	F_2	2625.1178	−2		
16	2	E	2431.2866	4			17	1	A_1	2518.2767	−2			17	12	F_2	2628.5078	−0		
16	3	E	2439.5132	−5			17	2	A_1	2530.2517	−8			17	13	F_2	2636.2299	8		
16	4	E	2439.9545	0			17	3	A_1	2571.2617	6			18	1	A_1	2613.0490	6		
16	6	E	2482.2886	3			17	4	A_1	2631.5799	3			18	2	A_1	2624.1503	−4		
16	8	E	2534.4963	−4			17	1	A_2	2518.2508	2			18	5	A_1	2669.1707	−1		
16	9	E	2540.9432	3			17	2	A_2	2529.0106	3			18	7	A_1	2729.5285	−2		
16	1	F_1	2430.0993	1			17	4	A_2	2574.7000	−3			18	1	E	2611.7287	1		
16	2	F_1	2439.3928	−2			17	5	A_2	2627.6268	−4			18	2	E	2624.0406	−3		
16	3	F_1	2439.8002	2			17	2	E	2529.0824	0			18	8	E	2728.4649	1		
16	4	F_1	2440.7533	0			17	3	E	2529.5791	3			18	1	F_1	2611.7328	−3		
16	6	F_1	2480.3351	−1			17	6	E	2570.5395	−2			18	9	F_1	2666.7402	6		
16	7	F_1	2480.8583	−7			17	7	E	2577.2430	−1			18	13	F_1	2728.8794	−5		
16	10	F_1	2530.7165	−4			17	9	E	2624.7085	1			18	14	F_1	2732.1391	4		
16	11	F_1	2536.6646	−1			17	10	E	2632.0738	1			18	10	F_2	2674.4906	−6		
16	12	F_1	2540.9738	4			17	1	F_1	2518.2665	−2			18	12	F_2	2727.1553	−7		
16	1	F_2	2430.0497	5			17	3	F_1	2529.0136	2			18	13	F_2	2732.3285	7		
16	2	F_2	2431.2627	−3			17	4	F_1	2529.1823	−0			19	1	A_1	2724.8992	1		
16	4	F_2	2439.4544	1			17	5	F_1	2529.7992	2			19	5	A_2	2837.9186	4		
16	5	F_2	2439.9320	−2			17	8	F_1	2570.7172	1			19	10	E	2832.1724	−3		
16	6	F_2	2472.6600	2			17	12	F_1	2624.2946	−4			19	14	F_1	2831.7919	−4		
16	6	F_2	2440.8036	−3			17	13	F_1	2629.1308	−3			19	15	F_1	2834.5667	4		
16	9	F_2	2479.7664	−4			17	14	F_1	2631.9361	3			19	13	F_2	2833.8554	−3		
16	10	F_2	2482.5816	3			17	15	F_1	2636.2641	7			19	14	F_2	2837.8099	7		
16	11	F_2	2485.3778	−1																

[a] In Table 6, δ is the difference $E^{exp.} - E^{calc.}$ in units of 10^{-4} cm^{-1}.

Table 7
Spectroscopic parameters $Y^{\Omega(K,n\Gamma)}_{v\gamma,v'\gamma'}$ of the set of interacting vibrational states (0200)/(0101)/(0020) in germane (in cm^{-1}).[a]

(v,γ) 1	(v',γ') 2	$\Omega(K,n\Gamma)$ 3	$^{76}GeH_4$ 4	$^{74}GeH_4$ 5
$(0200,A_1)$	$(0200,A_1)$	$0(0,A_1)$	−2.6836900(15)	−2.6836900
	$(0200,A_1)$	$2(0,A_1)10^3$	−0.4716(20)	−0.4716
$(0200,A_1)$	$(0200,E)$	$2(2,E)10^3$	−0.25523(48)	−0.25523
$(0200,E)$	$(0200,E)$	$0(0,A_1)$	0.8411139(99)	0.8411139
	$(0200,E)$	$2(2,E)10^3$	0.3393(20)	0.3393
	$(0200,E)$	$3(3,A_2)10^5$	0.26045(63)	0.26045
$(0200,A_1)$	$(0101,F_2)$	$2(2,F_2)10^3$	−0.1180(10)	−0.1180
$(0200,E)$	$(0101,F_1)$	$1(1,F_1)$	0.026348(93)	0.027471(12)
	$(0101,F_1)$	$2(2,F_2)10^3$	−0.21017(58)	−0.21017
	$(0101,F_1)$	$3(3,F_2)10^5$	−0.4234(17)	−0.4234
$(0200,E)$	$(0101,F_2)$	$1(1,F_1)$	0.031964(70)	0.0318184(94)
	$(0101,F_2)$	$3(1,F_1)10^5$	−0.4543(13)	−0.4543
$(0200,A_1)$	$(0002,A_1)$	$0(0,A_1)$	−5.4586(32)	−5.4586
	$(0002,A_1)$	$2(0,A_1)10^3$	0.5772(27)	0.5772
$(0200,E)$	$(0002,E)$	$0(0,A_1)$	0.1740(15)	0.1740
	$(0002,E)$	$2(2,E)10^3$	0.4579(13)	0.4579
$(0200,E)$	$(0002,F_2)$	$1(1,F_1)$	0.230860(96)	0.230860
	$(0002,F_2)$	$3(1,F_1)10^5$	−0.3016(27)	−0.3016
$(0101,F_1)$	$(0101,F_1)$	$0(0,A_1)$	2.2631000(96)	2.265386(13)
	$(0101,F_1)$	$1(1,F_1)$	−0.0510521(39)	−0.0510006(32)
	$(0101,F_1)$	$2(2,F_2)10^3$	−0.7694(21)	−0.7694
$(0101,F_1)$	$(0101,F_2)$	$1(1,F_1)$	−0.056359(15)	−0.0564421(24)
	$(0101,F_2)$	$2(2,E)10^4$	0.7774(15)	0.7774
	$(0101,F_2)$	$2(2,F_2)10^3$	0.79071(58)	0.79071
	$(0101,F_2)$	$3(1,F_1)10^5$	−0.58181(93)	−0.58181
$(0101,F_2)$	$(0101,F_2)$	$0(0,A_1)$	−2.013240(44)	−2.014151(13)
	$(0101,F_2)$	$1(1,F_1)$	−0.054986(58)	−0.054986
	$(0101,F_2)$	$2(0,A_1)10^3$	−0.37902(73)	−0.37902
	$(0101,F_2)$	$2(2,E)10^3$	0.3357(13)	0.3357
	$(0101,F_2)$	$2(2,F_2)10^3$	−0.8515(11)	−0.8515
	$(0101,F_2)$	$3(1,F_1)10^4$	−0.18456(29)	−0.18456
	$(0101,F_2)$	$3(3,F_1)10^4$	−0.14931(17)	−0.14931
$(0101,F_1)$	$(0002,A_1)$	$1(1,F_1)$	0.065933(82)	0.66456(11)
$(0101,F_1)$	$(0002,F_2)$	$2(2,E)10^3$	0.15190(89)	0.15190
	$(0002,F_2)$	$3(3,A_2)10^5$	0.3359(20)	0.3359
	$(0002,F_2)$	$3(3,F_1)10^5$	−0.9951(23)	−0.9951
$(0101,F_2)$	$(0002,A_1)$	$2(2,F_2)10^3$	0.3879(15)	0.3879
	$(0002,A_1)$	$3(3,F_2)10^5$	−0.2500(31)	−0.2500
$(0101,F_2)$	$(0002,E)$	$3(1,F_1)10^4$	−0.12605(34)	−0.12605
$(0101,F_2)$	$(0002,F_2)$	$0(0,A_1)$	−4.29715(54)	−4.299864(32)
	$(0002,F_2)$	$1(1,F_1)$	0.025605(25)	0.253294(59)
	$(0002,F_2)$	$2(0,A_1)10^3$	0.63352(73)	0.63352
	$(0002,F_2)$	$2(2,E)10^4$	−0.2856(79)	−0.2856
	$(0002,F_2)$	$3(1,F_1)10^5$	−0.2178(17)	−0.2178
	$(0002,F_2)$	$3(3,F_2)10^4$	0.14725(28)	0.14725
$(0002,A_1)$	$(0002,A_1)$	$0(0,A_1)$	−13.02924(16)	−13.02924
$(0002,A_1)$	$(0002,E)$	$2(2,E)10^3$	0.21603(72)	0.21603
$(0002,A_1)$	$(0002,F_2)$	$2(2,F_2)10^3$	−0.28757(91)	−0.28757
	$(0002,F_2)$	$3(3,F_2)10^4$	0.10986(73)	0.10986
$(0002,E)$	$(0002,E)$	$0(0,A_1)$	1.488348(27)	1.488348
	$(0002,E)$	$2(2,E)10^3$	−0.5182(15)	−0.5182
	$(0002,E)$	$3(3,A_2)10^4$	0.10591(30)	0.10591
$(0002,E)$	$(0002,F_2)$	$1(1,F_1)$	0.0302266(28)	0.0302266
	$(0002,F_2)$	$2(2,F_2)10^3$	−0.59615(66)	−0.59615
	$(0002,F_2)$	$3(3,F_1)10^5$	−0.1960(11)	−0.1960
	$(0002,F_2)$	$3(3,F_2)10^5$	−0.5111(19)	−0.5111
$(0002,F_2)$	$(0002,F_2)$	$0(0,A_1)$	−1.227540(43)	−1.227540
	$(0002,F_2)$	$1(1,F_1)$	−0.032705(58)	−0.032705
	$(0002,F_2)$	$2(0,A_1)10^4$	−0.1478(46)	−0.1478

Table 7 (*continued*)

(v,γ) 1	(v',γ') 2	$\Omega(K,n\Gamma)$ 3	$^{76}GeH_4$ 4	$^{74}GeH_4$ 5
	$(0002,F_2)$	$2(2,E)10^3$	0.1190(12)	0.1190
	$(0002,F_2)$	$2(2,F_2)10^3$	0.58023(98)	0.58023
	$(0002,F_2)$	$3(3,F_1)10^5$	−0.5775(37)	−0.5775

[a] Values in parentheses are 1σ statistical confidence intervals. Parameters of $^{74}GeH_4$ presented in column 5 without confidence intervals were constrained to the values of corresponding parameters of the $^{76}GeH_4$ isotopologue and were fixed in the fit.

Table 8
Spectroscopic parameters $Y^{\Omega(K,n\Gamma)}_{v_\gamma,v'_{\gamma'}}$ of the ground vibrational state of germane (in cm^{-1}).[a]

$\Omega(K,n\Gamma)$ 1	$^{76}GeH_4$ 2	$^{74}GeH_4$ 3
$2(0,A_1)$	2.695870305	2.695864734
$4(0,A_1)10^4$	−0.3341682	−0.3341682
$4(4,A_1)10^5$	−0.1547079	−0.1547079
$6(0,A_1)10^8$	0.114368	0.114368
$6(4,A_1)10^{10}$	−0.51075	−0.51075
$6(6,A_1)10^{10}$	−0.15638	−0.15638

[a] The $(v\gamma)=(v'\gamma')=(0000,A_1)$.

summation in Eq. (11) is fulfilled in all degenerate and/or interacting vibrational states. For different type polyatomic molecules the operators $H^{a,b}$ have a specific form which depends on a symmetry of a molecule (see, e.g., Refs. [58–65]). In its turn, for the T_d-symmetry type molecules, the most efficiently the effective Hamiltonian can be written in the following form:

$$H^{vib.-rot.} = \sum_{v\gamma,v'\gamma'}\sum_{n\Gamma}\left[(|v\gamma\rangle\otimes\langle v'\gamma'|)^{n\Gamma}\otimes H^{n\Gamma}_{v\gamma,v'\gamma'}\right]^{A_1} \equiv \sum_{v\gamma,v'\gamma'}\sum_{n\Gamma}\sum_{\Omega K}\left[(|v\gamma\rangle\otimes\langle v'\gamma'|)^{n\Gamma}\otimes R^{\Omega(K,n\Gamma)}\right]^{A_1} Y^{\Omega(K,n\Gamma)}_{v\gamma,v'\gamma'}. \quad (11)$$

Here $|v\gamma\rangle$ are the above discussed symmetrized vibrational functions; operators $R^{\Omega(K,n\Gamma)}_\sigma$ are determined above; and $Y^{\Omega(K,n\Gamma)}_{v\gamma,v'\gamma'}$ are spectroscopic parameters. In this case, when $v=v'$ and $\gamma=\gamma'$, the parameters $Y^{\Omega(K,n\Gamma)}_{v\gamma,v\gamma}$ describe the rotational structure of the vibrational state $(v\gamma)$. If $\gamma=\gamma'$, but $v\neq v'$, the parameters $Y^{\Omega(K,n\Gamma)}_{v\gamma,v'\gamma}$ describe Fermi-type interactions. If $\gamma\neq\gamma'$ (v and v' are arbitrary), the parameters $Y^{\Omega(K,n\Gamma)}_{v\gamma,v'\gamma'}$ describe Coriolis-type interactions.

5. Analysis of the ro-vibrational structure of the doubly excited vibrational states $(v_4=2)$, $(v_2=v_4=1)$, and $(v_2=2)$

As was discussed in Section 3, about 2260 transitions with the maximum values of upper quantum numbers $J^{max.}$ equal to 15, 13, 19, 18, 19, and 18 were assigned to the six ($2\nu_4(F_2)$, $2\nu_4(E)$, $\nu_2+\nu_4(F_1)$, $\nu_2+\nu_4(F_2)$, $2\nu_2(E)$, and $2\nu_2(A_1)$, respectively) sub-bands of the $2\nu_4$, $\nu_2+\nu_4$ and $2\nu_2$ bands of the $^{76}GeH_4$ molecule. Additionally, about 1000 "hot" transitions from the $(v_4=1,F_2)$ and $(v_2=1,E)$ vibrational states to six $(v_4=2,F_2)$, $(v_4=2,E)$, $(v_4=2,A_1)$, $(v_4=v_2=1,F_2)$, $(v_4=v_2=1,F_1)$, and $(v_2=2,E)$ vibrational states were assigned in the dyad spectral region. As a result, for the first time 1272 ro-vibrational energies of the seven above mentioned upper vibrational states were determined. It is necessary to note that in this analysis we were not able to assign transitions belonging to the $2\nu_4(A_1)$ band. At the same time, 76 transitions were assigned to the "hot" $2\nu_4(A_1)-\nu_4$ band. That gave us possibility to determine 29 ro-vibrational energies of the $(v_4=2,A_1)$ vibrational state. Lists of obtained upper ro-vibrational energies are presented in columns 2 and 4 of Tables 3–6 (for more details, see statistical information in Table 2).

The obtained values of upper energies were used then in the weighted fit procedure with the Hamiltonian (11) on

Table 9
Spectroscopic parameters $Y^{\Omega(K,n\Gamma)}_{v_\gamma,v'_{\gamma'}}$ of the $(0100,E)$, $(0001,F_2)$, and the $(0100,E)/(0001,F_2)$ Coriolis interaction of germane (in cm^{-1}).

(v,γ) 1	(v',γ') 2	$\Omega(K,n\Gamma)$ 3	$^{76}GeH_4$ 4	$^{74}GeH_4$ 5
$(0100,E)$	$(0100,E)$	$0(0,A_1)$	929.91303	929.90931
		$2(2,E)10^2$	−1.078743	−1.0788781
		$3(3,A_2)10^4$	0.22618	0.22618
		$4(0,A_1)10^6$	−0.4052	−0.4052
		$4(2,E)10^6$	−0.31077	−0.31077
		$4(4,A_1)10^7$	0.134	0.134
		$4(4,E)10^6$	−0.12583	−0.12583
$(0100,E)$	$(0010,F_2)$	$1(1,F_1)$	−4.503062	−4.506095
		$2(2,F_2)10^2$	−2.131680	−2.130080
		$3(1,F_1)10^3$	−0.1179267	−0.1179267
		$3(3,F_2)10^4$	0.138096	0.138096
		$4(2,F_2)10^6$	−0.2122	−0.2122
		$4(4,F_1)10^6$	−0.18552	−0.18552
		$4(4,F_2)10^6$	−0.209879	−0.209879
		$5(1,F_1)10^8$	−0.23013	−0.23013
		$5(3,F_1)10^8$	0.13677	0.13677
		$5(5,F_1)10^9$	0.5885	0.5885
$(0010,F_2)$	$(0010,F_2)$	$0(0,A_1)$	820.32700	820.71185
		$1(1,F_1)$	6.391862	6.385349
		$2(0,A_1)10^2$	0.10604550	0.10672896
		$2(2,E)10^2$	−0.1484110	−0.1498614
		$2(2,F_2)10^2$	−1.06923	−1.06946
		$3(1,F_1)10^4$	0.70545	0.70479
		$3(3,F_1)10^4$	−0.47902	−0.47902
		$4(0,A_1)10^4$	−0.3653	−0.3653
		$4(2,F_2)10^6$	−0.3519	−0.3519
		$4(4,A_1)10^7$	−0.6407	−0.6407
		$5(1,F_1)10^8$	0.25953	0.25953
		$5(3,F_1)10^8$	−0.1697	−0.1697
		$6(0,A_1)10^{10}$	0.4276	0.4276

Table 10
Ro-vibrational term values for the $(0101, F_1)$ vibrational state of the $^{74}GeH_4$ molecule (in cm^{-1}).[a]

J	n	γ	E(0101,F1)	δ	J	n	γ	E(0101,F1)	δ	J	n	γ	E(0101,F1)	δ	J	n	γ	E(0101,F1)	δ	J	n	γ	E(0101,F1)	δ
1			2	3	1			2	3	1			2	3	1			2	3	1			2	3
1	1	E	1759.7396	−4	5	3	F_1	1846.2079	1	7	2	F_2	1900.4092	4	9	2	E	1993.0008	4	10	1	F_2	2014.2744	2
1	1	F_2	1759.0519	−2	5	4	F_1	1847.9350	2	7	3	F_2	1901.2256	−5	9	4	E	2019.4731	−3	10	2	F_2	2014.6619	−4
2	1	A_2	1766.1846	3	5	1	F_2	1813.8885	1	7	4	F_2	1902.6408	−1	9	1	F_1	1963.4408	5	10	3	F_2	2044.5636	−1
2	1	E	1773.2971	2	5	3	F_2	1846.4605	−4	7	5	F_2	1923.0508	2	9	3	F_1	1993.2850	−1	10	5	F_2	2047.5696	−1
2	1	F_1	1773.0861	−2	5	4	F_2	1847.3664	1	7	6	F_2	1923.8957	0	9	5	F_1	2019.7911	1	10	7	F_2	2075.6398	3
2	1	F_2	1765.1644	0	6	1	A_1	1881.0320	1	8	1	A_1	1944.3972	−3	9	6	F_1	2021.2536	−2	11	1	A_1	2071.0787	−5
2	2	F_2	1773.7115	1	6	1	A_2	1843.0766	0	8	1	A_2	1946.8268	−4	9	1	F_2	1963.4482	−1	11	2	A_1	2112.0211	4
3	1	A_1	1771.4048	0	6	1	E	1862.3504	0	8	2	A_2	1969.1497	−4	9	2	F_2	1963.7839	−3	11	3	A_1	2138.0478	2
3	1	A_2	1792.6104	−1	6	3	E	1882.5363	0	8	1	E	1917.9326	3	9	3	F_2	1991.7632	−6	11	2	A_2	2140.0243	−3
3	1	F_1	1781.1975	0	6	1	F_1	1843.3503	−1	8	3	E	1944.7245	−2	9	4	F_2	1993.5545	3	11	1	E	2070.5282	2
3	2	F_1	1792.2148	0	6	3	F_1	1881.1340	0	8	4	E	1966.7832	2	9	6	F_2	2017.3180	0	11	1	F_1	2070.4550	3
3	2	F_2	1792.3432	0	6	4	F_1	1882.4287	0	8	5	E	1968.6798	−2	9	7	F_2	2019.3811	3	11	6	F_1	2137.2420	5
4	1	A_1	1803.0165	3	6	2	F_2	1862.5932	2	8	1	F_1	1917.9383	−3	10	1	A_1	2047.6896	−3	11	1	F_2	2070.5995	2
4	1	A_2	1817.6257	1	6	4	F_2	1881.2944	−2	8	2	F_1	1918.3003	−4	10	2	A_1	2076.0154	6	11	2	F_2	2070.8145	1
4	2	E	1816.6393	0	6	5	F_2	1883.0878	1	8	3	F_1	1943.4088	0	10	1	A_2	2014.5188	−2	11	5	F_2	2107.1915	0
4	1	F_1	1789.9608	0	7	1	A_1	1878.1711	0	8	4	F_1	1944.5832	−2	10	3	A_2	2075.5185	−3	11	8	F_2	2137.0082	−2
4	2	F_1	1802.6882	0	7	2	A_1	1922.6831	0	8	6	F_1	1968.4107	0	10	1	E	2014.3097	0	12	1	A_2	2132.3300	0
4	4	F_1	1816.6988	1	7	1	A_2	1900.8586	5	8	7	F_1	1970.0059	4	10	3	E	2046.6146	−3	12	1	E	2132.4960	2
4	5	F_1	1818.1108	4	7	2	A_2	1923.5232	1	8	2	F_2	1944.2727	−1	10	5	E	2076.8800	3	12	2	F_1	2132.4755	0
4	1	F_2	1816.6400	−4	7	3	A_2	1924.0066	2	8	4	F_2	1966.6203	5	10	1	F_1	2014.3337	1	12	3	F_1	2132.6971	2
4	2	F_2	1817.9325	1	7	2	E	1921.3954	−2	8	5	F_2	1968.8100	−5	10	2	F_1	2014.7572	−1	12	2	F_2	2132.6035	−7
5	1	A_1	1831.4129	−1	7	1	F_1	1878.1307	−1	8	6	F_2	1969.7575	0	10	3	F_1	2047.3857	2	13	1	A_1	2199.5089	5
5	1	E	1813.9583	−3	7	2	F_1	1900.2267	2	9	1	A_1	1963.4450	0	10	5	F_1	2051.2463	−2	13	3	A_1	2245.0291	1
5	2	E	1846.2573	−1	7	4	F_1	1921.2216	1	9	3	A_1	2021.4409	−1	10	6	F_1	2075.7800	1	13	1	A_2	2199.5072	5
5	3	E	1847.8298	1	7	5	F_1	1922.8652	−3	9	1	A_2	1963.5284	−2	10	7	F_1	2076.7260	7	13	2	F_1	2199.4952	4
5	1	F_1	1830.0095	1	7	1	F_2	1877.8083	2	9	2	A_2	2017.1577	−1	10	8	F_1	2078.0442	−4						

[a] In Table 10, δ is the difference $E^{exp.} - E^{calc.}$ in units of 10^{-4} cm^{-1}.

the basis of the SPHETOM Fortran code, Ref. [32]. A set of 62 varied parameters (25 parameters of the diagonal blocks and 37 resonance interaction parameters) was obtained from the fit. Taking into account that the most of the readers are more familiar with the XTDS software developed in Dijon, Ref. [66], than with the SPHETOM Fortran code, values of spectroscopic parameters obtained in our study were recalculated to the values of corresponding parameters used in the XTDS code (connections between the parameters of SPHETOM and XTDS can be found, e.g., in Table 5 of our recent paper, Ref. [33]). Namely these values are presented in column 4 of Table 7 together with their 1σ statistical confidence intervals (the lasts are shown in parentheses). Practical use of the data from Table 7 requires also knowledge of parameters of both the ground vibrational state and of the $(v_2 = 1)/(v_4 = 1)$ dyad determined in our earlier study, Ref. [32]. For convenience of the reader, these data are reproduced from Ref. [32] in Tables 8 and 9. The obtained from the fit set of 62 parameters reproduces the 1272 initial values of "experimental" ro-vibrational energies with the d_{rms} ("cold" bands)=2.6 $\times 10^{-4}$ cm^{-1} and d_{rms}("hot" bands)= 2.9 $\times 10^{-4}$ cm^{-1}, which are close to the experimental uncertainties. This can be considered as a good confirmation of the results correctness. Also for illustration, column 9 of Supplementary Material I and columns 3 and 5 of Tables 3–6 present the differences δ (in units 10^{-4} cm^{-1}) between experimental and calculated values. One can see more than satisfactory correspondence between the calculated and the experimental data.

Analysis of the experimental data for the $^{74}GeH_4$ molecule was made analogous to $^{76}GeH_4$. In this case, 408 assigned experimental transitions (309 "cold" and 99 "hot" transitions with the value $J_{max} = 15$) gave us possibility to obtain 285 upper ro-vibrational energy levels which are presented in column 2 of Tables 10 and 11. The use of these values in the fit procedure was made analogous to the $^{76}GeH_4$ species. In this case, only 9 parameters were fitted. Values of all other parameters were fixed to the values of the corresponding parameters of the $^{76}GeH_4$ molecule (additional fitting of any of them did not improve the result). The parameters obtained from the fit are shown in column 5 of Table 7 together with their 1σ statistical confidence intervals. One can see that the values of the fitted parameters of $^{74}GeH_4$ are very close to the values of the corresponding parameters of $^{76}GeH_4$ (this fact is the consequence of a very small value of the ratio $\frac{(M(76)-M(74))}{M(76)}$). The obtained set of parameters reproduces the 285 "experimental" energy values of the $^{74}GeH_4$ molecule with $d_{rms}^{cold} = 2.7 \times 10^{-4}$ cm^{-1} and $d_{rms}^{hot} = 2.9 \times 10^{-4}$ cm^{-1}.

As an additional illustration of correctness of the obtained results, Fig. 4 shows the fit residuals for line positions as a function of the quantum number J. Fig. 5 presents a diagram of the reduced energy levels of $^{76}GeH_4$ for the studied upper vibrational states as defined by the equation

$$E_{Jn\gamma}^{red.}/hc = E_{Jn\gamma}/hc - B_{gr}J(J+1) + D_{gr}J^2(J+1)^2 - \ldots \quad (12)$$

Simulation of the spectrum in the region of the studied "cold" bands is presented at the bottom of Figs. 1 and 2 and illustrates good agreement between experimental and

Table 11
Ro-vibrational term values for the $(0101, F_2)$ vibrational state of the $^{74}GeH_4$ molecule (in cm^{-1}).[a]

J	n	γ	$E(0101,F_2)$	δ	J	n	γ	$E(0101,F_2)$	δ	J	n	γ	$E(0101,F_2)$	δ	J	n	γ	$E(0101,F_2)$	δ	J	n	γ	$E(0101,F_2)$	δ
1			2	3	1			2	3	1			2	3	1			2	3	1				
0	1	F_2	1748.7771	−2	5	1	F_1	1813.0677	0	7	5	F_2	1924.3825	1	10	2	E	2016.1697	3	12	1	A_2	2135.8714	0
1	1	A_2	1757.9112	3	5	2	F_1	1813.2026	1	8	1	A_1	1917.1296	0	10	5	E	2081.7955	−1	12	3	A_2	2200.5814	−1
1	1	E	1749.5513	1	5	3	F_1	1825.8115	−1	8	3	A_1	1971.9528	−1	10	1	F_1	2013.5703	4	12	2	E	2135.8924	3
1	1	F_2	1753.6937	2	5	4	F_1	1847.5374	2	8	1	A_2	1917.3347	2	10	2	F_1	2016.2113	0	12	6	E	2213.2201	1
2	1	A_1	1761.3404	1	5	1	F_2	1813.1213	0	8	3	E	1971.1112	−3	10	3	F_1	2016.8925	−4	12	1	F_1	2131.2699	−2
2	1	F_1	1757.5764	−2	5	2	F_2	1826.2512	1	8	1	F_1	1917.1922	2	10	7	F_1	2079.0291	−3	12	2	F_1	2135.5257	3
2	2	F_2	1772.8642	−1	5	4	F_2	1848.7778	−1	8	2	F_1	1918.9169	−2	10	8	F_1	2084.9584	0	12	6	F_1	2209.6834	−3
3	1	A_1	1792.4277	−1	6	1	A_1	1842.7824	2	8	5	F_1	1971.4475	1	10	1	F_2	2013.4374	3	12	7	F_1	2213.3753	−1
3	1	A_2	1770.2303	0	6	2	A_1	1857.5105	5	8	6	F_1	1974.0754	−2	10	2	F_2	2016.0505	2	12	8	F_1	2217.4733	5
3	1	E	1770.5378	2	6	1	E	1842.4180	−2	8	1	F_2	1917.2604	1	10	3	F_2	2016.9092	−6	12	1	F_2	2131.2194	7
3	2	E	1780.7300	2	6	3	E	1883.4383	2	8	3	F_2	1918.9646	−2	10	6	F_2	2079.5289	−1	12	2	F_2	2135.5705	1
3	3	E	1792.7473	2	6	1	F_1	1842.4479	0	8	6	F_2	1970.3494	0	10	7	F_2	2081.5993	0	12	3	F_2	2135.8857	−2
3	1	F_1	1770.8651	−3	6	2	F_1	1842.8926	−4	8	7	F_2	1974.1916	−1	10	8	F_2	2085.0178	0	12	11	F_2	2210.9901	−2
3	2	F_1	1777.8730	−4	6	4	F_1	1862.0180	4	9	1	A_1	1965.1469	−3	11	1	A_1	2069.7723	3	12	12	F_2	2217.4978	0
3	3	F_1	1792.6698	−2	6	5	F_1	1884.9650	−1	9	1	A_2	1964.5505	1	11	3	A_1	2148.5022	2	13	2	A_1	2282.8412	−3
3	1	F_2	1770.3582	−1	6	1	F_2	1842.4333	0	9	3	A_2	2026.9266	1	11	1	A_2	2069.6105	4	13	1	A_2	2203.5798	2
3	2	F_2	1779.1525	0	6	2	F_2	1842.9528	−1	9	1	E	1962.6829	1	11	4	A_2	2142.9968	1	13	4	A_2	2280.8716	−6
4	1	A_1	1817.1830	1	6	3	F_2	1860.4124	5	9	2	E	1965.1978	−5	11	5	E	2141.5923	0	13	8	E	2284.5415	−4
4	1	A_2	1800.6057	−1	6	4	F_2	1883.2669	3	9	5	E	2026.8025	0	11	6	E	2148.5619	4	13	9	F_1	2284.2382	−2
4	1	E	1789.1466	2	6	5	F_2	1885.1852	1	9	1	F_1	1962.6077	3	11	1	F_1	2069.7061	1	13	10	F_1	2287.4586	2
4	2	E	1799.2148	−1	7	2	A_1	1926.6883	−2	9	2	F_1	1964.6394	3	11	3	F_1	2073.3240	−1	13	3	F_2	2203.5510	0
4	1	F_1	1789.0109	−2	7	1	A_2	1878.2426	−1	9	3	F_1	1965.1821	−3	11	8	F_1	2140.8663	−2	13	9	F_2	2281.3062	1
4	2	F_1	1817.8435	0	7	1	E	1877.1468	3	9	7	F_1	2021.9581	−1	11	9	F_1	2144.9375	1	13	10	F_2	2287.2368	0
4	1	F_2	1788.9837	1	7	2	E	1877.9596	−1	9	1	F_2	1962.7516	−4	11	10	F_1	2148.5424	2	14	10	F_2	2359.0550	−2
4	2	F_2	1789.3130	0	7	3	E	1878.2081	0	9	2	F_2	1964.5945	−1	11	1	F_2	2069.6545	4	15	6	A_2	2448.0409	−5
4	3	F_2	1799.4983	3	7	5	E	1926.9523	0	9	5	F_2	2023.4134	0	11	2	F_2	2073.2710	0	15	8	E	2447.2810	5
4	4	F_2	1802.1658	0	7	4	F_1	1898.2914	1	9	6	F_2	2026.8465	−1	11	4	F_2	2095.7219	−4	15	11	F_2	2447.5816	−1
4	5	F_2	1818.0717	−1	7	5	F_1	1924.7932	3	10	1	A_1	2016.2720	−2	11	5	F_2	2134.3732	−1	15	12	F_2	2451.3204	7
5	1	A_1	1813.0512	1	7	6	F_1	1926.8778	1	10	2	A_1	2037.5544	−1	11	6	F_2	2142.0453	−1					
5	1	A_2	1813.2295	−1	7	1	F_2	1877.1905	0	10	3	A_1	2078.5215	1	11	7	F_2	2144.5997	−2					
5	3	A_2	1848.9777	1	7	2	F_2	1878.1971	1	10	2	A_2	2080.9317	0	12	1	A_1	2135.4742	1					
5	3	E	1848.6418	2	7	4	F_2	1921.6007	1	10	1	E	2013.4886	−1	12	3	A_1	2213.6272	0					

[a] In Table 11, δ is the difference $E^{exp.} - E^{calc.}$ in units of 10^{-4} cm^{-1}.

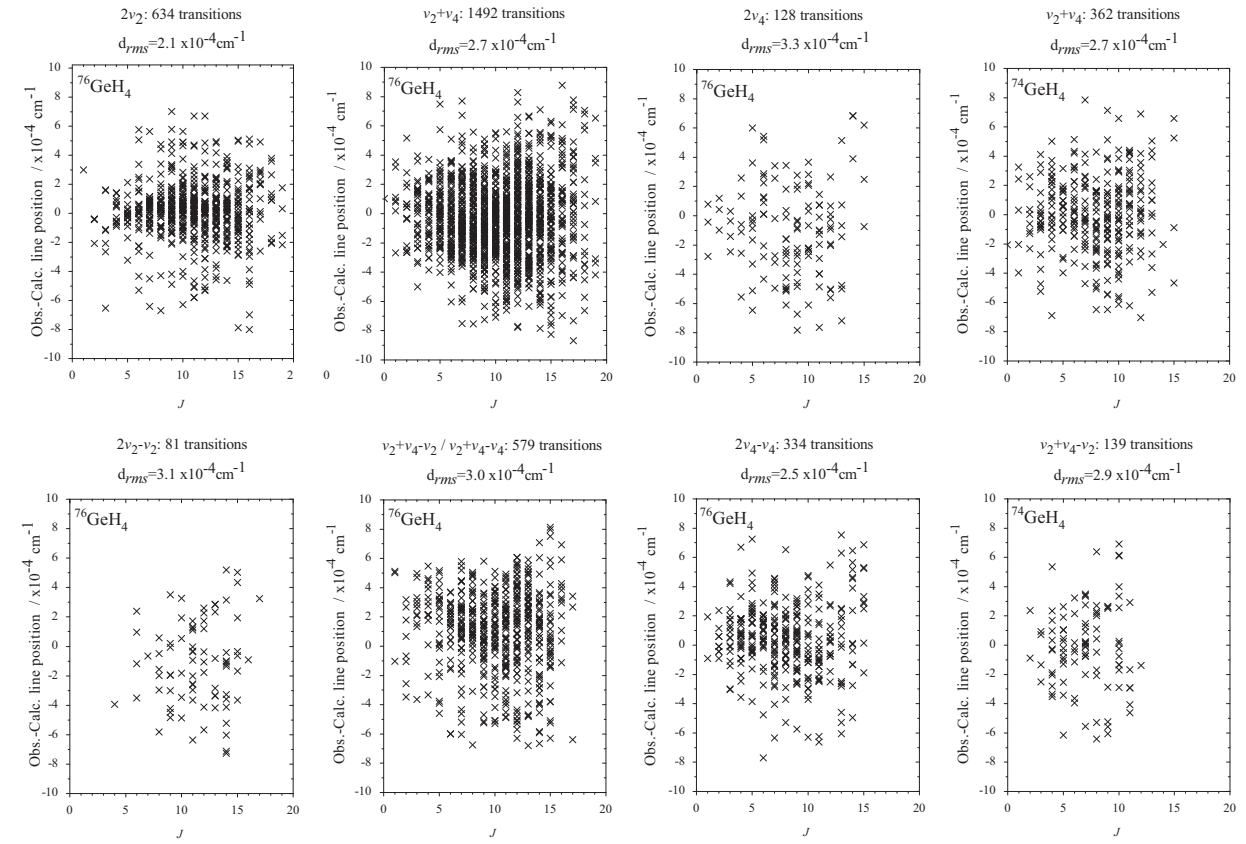

Fig. 4. Observed calculated line positions and fit statistics for the bands of $^{76}GeH_4$ and $^{74}GeH_4$ studied in the present paper.

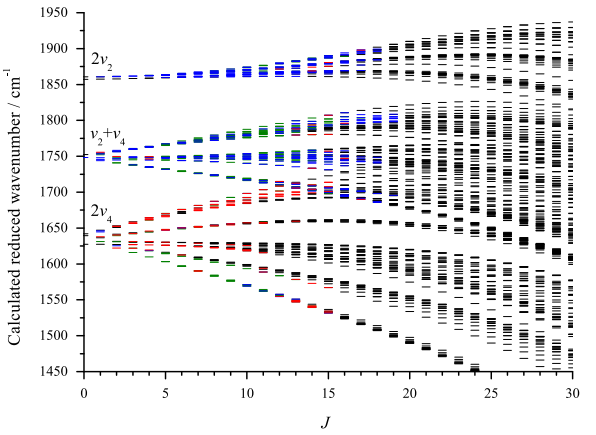

Fig. 5. Reduced ro-vibrational energy levels for the $2\nu_4$, $\nu_2+\nu_4$, and $2\nu_2$ bands of $^{76}GeH_4$. Energy levels obtained only from the "cold" transitions, or only from the "hot" transitions are marked by blue and red, respectively. Energy levels marked by green were obtained both from the "cold", and from the "hot" transitions. Energy levels marked by black are the levels calculated with the parameters of the present paper. (For interpretation of the references to color in this figure caption, the reader is referred to the web version of this paper.)

synthetic spectra. In this case, we calculated the relative line intensities, and only one main effective dipole moment parameter for any of the three bands ($\nu_3(F_2)$, $\nu_2+\nu_4(F_2)$, and $2\nu_4(F_2)$) allowed by the symmetry of the molecule was used: 1 for the $\nu_3(F_2)$ band, $3/4\times10^{-1}$ for the $\nu_2+\nu_4(F_2)$ band, and $1/3\times10^{-2}$ for the $2\nu_4(F_2)$ band. Calculation schemes from Refs. [67,68] and Doppler profile of the lines were used in calculations.

6. Conclusion

The high resolution Fourier transform spectra of the $^{76}GeH_4$ molecule in the region of the $2\nu_4(F_2)$, $2\nu_4(E)$, $2\nu_4(A_1)$, $\nu_2+\nu_4(F_2)$, $\nu_2+\nu_4(F_1)$, $2\nu_2(A_1)$ and $2\nu_2(E)$ bands were recorded with a high resolution under different experimental conditions and were analyzed theoretically. As a result of analysis, 2254 transitions with $J^{max.}=19$ were assigned for the first time to these bands. About 1000 "hot Dyad–Pentad" transitions were also recorded and assigned for the first time in the region of 700–1080 cm^{-1}. Rotational, centrifugal distortion, tetrahedral splitting, and interaction parameters for the $(0002,F_2)$, $(0002,E)$, $(0002,A_1)$, $(0101,F_2)$, $(0101,F_1)$, $(0200,A_1)$ and $(0200,E)$ vibrational states were determined from the fit of experimental line positions. Analogous analysis of the $^{74}GeH_4$ isotopologue gave us possibility to assign 309 "cold" and 99 "hot" transitions which were also used in the fit procedure for determination of spectroscopic parameters. The obtained sets of spectroscopic parameters reproduce the initial experimental data with the accuracy close to the experimental uncertainties.

Acknowledgments

The work was supported by the project "Leading Russian Research Universities" (Grant FTI-24/2016 of the Tomsk Polytechnic University, Russia). Part of the work was supported by the Russian Foundation of Basic Researches (Grant nos. 16-32-00305 mol_a and 15–02–07887).

Appendix A. Supplementary data

Supplementary data associated with this paper can be found in the online version at http://dx.doi.org/10.1016/j.jqsrt.2016.05.014.

References

[1] Fink U, Larson HP, Treffers RR. Germane in the atmosphere of Jupiter. Icarus 1978;34:344–54.
[2] Chen F, Judge DL, Wu CYR, Caldwell J, White HP, Wagener R. High-resolution low-temperature Photoabsorption Cross Sections of C_2H_2, PH_3, AsH_3, and GeH_4, with application to Saturn's atmosphere. J Geophys Res 1991;96:17519–27.
[3] Atreya SK, Mahaffy PR, Niemann HB, Wong MH, Owen TC. Composition and origin of the atmosphere of Jupiter an update, and implications for the extrasolar giant planets. Planet Space Sci 2003;51:105–12.
[4] Lodders K. Jupiter formed with more tar than ice. Astrophys J 2004;611:587–97.
[5] Lodders K. Atmospheric chemistry of the gas giant planets. Geochem Soc 2010 ⟨http://www.geochemsoc.org/publications/geochemicalnews/gn142jan10/atmosphericchemistryoftheg/⟩.
[6] Haller EE. Germanium: from its discovery to SiGe devices. Mater Sci Semicond Process 2006;9:408–22.
[7] Agostini M, Allardt M, Andreotti E, Bakalyarov AM, Balata M, Barabanov I, et al. The background in the $0\nu\beta\beta$ experiment GERDA. Eur Phys J 2014;74 2764_1–25.
[8] Curl RF, Oka T, Smith DS. The observation of a pure rotational Q-branch transition of methane by infrared-radio frequency double resonance. J Mol Spectrosc 1973;46:518–20.
[9] Curl Jr RF. Infrared-radio frequency double resonance observations of pure rotational Q-branch transitions of methane. J Mol Spectrosc 1973;48:165–73.
[10] Kreiner WA, Oka T. Infrared-radio-frequency double resonance observations of $\Delta J = 0$ Forbidden rotational transitions of SiH_4. Can J Phys 1975;53:2000–6.
[11] Kreiner WA, Andresen U, Oka T. Infrared-microwave double resonance spectroscopy of GeH_4. J Chem Phys 1977;66:4662–5.
[12] Kreiner WA, Orr BJ, Andresen U, Oka T. Measurement of the centrifugal-distortion dipole moment of GeH_4 using a CO_2 laser. Phys Rev A 1977;15:2298–304.
[13] Kagann RH, Ozier I, Gerry MCL. The centrifugal distortion dipole moment of silane. J Chem Phys 1976;64:3487–8.
[14] Lepage P, Brégier R, Saint-Loup R. La bande ν_3 du germane. C R Acad Sci Ser B 1976;B283:179–80.
[15] Kagann RH, Ozier I, McRae GA, Gerry MCL. The distortion moment spectrum of GeH_4: the microwave Q branch. Can J Phys 1979;57:593–600.
[16] Daunt SJ, Halsey GW, Fox K, Lovell RJ, Gailar NM. High-resolution infrared spectra of ν_3 and $2\nu_3$ of germane. J Chem Phys 1978;68:1319–21.
[17] Fox K, Halsey GW, Daunt SJ, Kennedy RC. Transition moment for ν_3 of $^{74}GeH_4$. J Chem Phys 1979;70:5326–7.
[18] Kreiner WA, Magerl G, Furch B, Bonek E. IR laser sideband observations in GeH_4 and CD_4. J Chem Phys 1979;70:5016–20.
[19] Magerl G, Schupita W, Bonek E, Kreiner WA. Observation of the isotope effect in the ν_2 fundamental of germane. J Chem Phys 1980;72:395–8.
[20] Kreiner WA, Opferkuch R, Robiette AG, Turner PH. The ground-state rotational constants of germane. J Mol Spectrosc 1981;85:442–8.
[21] Lepage P, Champion JP, Robiette AG. Analysis of the ν_3 and ν_1 infrared bands of GeH_4. J Mol Spectrosc 1981;89:440–8.
[22] Cheglokov AE, Kuritsin YuA, Snegirev EP, Ulenikov ON, Vedeneeva GV. High-resolution spectroscopy of the ν_2 Q Branch of GeH_4, with a computer-assisted, pulsed-diode laser spectrometer. J Mol Spectrosc 1984;105:385–96.
[23] Cheglokov AE, Kuritsin YuA, Snegirev EP, Ulenikov ON, Vedeneeva GV. Study of the ν_2 infrared band of GeH_4: Q-branch. Mol Phys 1984;53:287–94.
[24] Schaeffer RD, Lovejoy RW. Absolute line strengths of $^{74}GeH_4$ near 5 μm. J Mol Spectrosc 1985;113:310–4.
[25] Zhu Q, Thrush BA, Robiette AG. Local mode rotational structure in the (3000) Ge–H stretching overtone ($3\nu_3$) of germane. Chem Phys Lett 1988;150:181–3.
[26] Zhu Q, Thrush BA. Rotational structure near the local mode limit in the (3000) band of germane. J Chem Phys 1990;92:2691–7.
[27] Zhu Q, Qian H, Thrush BA. Rotational analysis of the (2000) and (3000) bands and vibration–rotation interaction in germane local mode states. Chem Phys Lett 1991;186:436–40.
[28] Campargue A, Vetterhöffer J, Chenevier M. Rotationally resolved overtone transitions of $^{70}GeH_4$ in the visible and near-infrared. Chem Phys Lett 1992;192:353–6.
[29] Zhu Q, Campargue A, Vetterhöffer J, Permogorov D, Stoeckel F. High resolution spectra of GeH_4 v=6 and 7 stretch overtones. The perturbed local mode vibrational states. J Chem Phys 1993;99:2359–64.
[30] Sun F, Wang X, Liao J, Zhu Q. The (5000) local mode vibrational state of germane: a high-resolution spectroscopic study. J Mol Spectrosc 1997;184:12–21.
[31] Chen XY, Lin H, Wang XG, Deng K, Zhu QS. High-resolution fourier transform spectrum of the (4000) local mode overtone of GeH_4: local mode effect. J Mol Struct 2000;517–518:41–51.
[32] Ulenikov ON, Gromova OV, Bekhtereva ES, Raspopova NI, Sennikov PG, Koshelev MA, et al. High resolution study of $^{M}GeH_4$ ($M = 76, 74$) in the dyad region. J Quant Spectrosc Radiat Transf 2014;144:11–26.
[33] Koshelev MA, Velmuzhov AP, Velmuzhova IA, Sennikov PG, Raspopova NI, Bekhtereva ES, et al. High resolution study of strongly interacting $\nu_1(A_1)/\nu_3(F_2)$ bands of $^{M}GeH_4$ ($M = 76, 74$). J Quant Spectrosc Radiat Transf 2015;164:161–74.
[34] Rothman LS, Gordon IE, Babikov Y, Benner DC, Bernath PF, Birk M, et al. The HITRAN2012 molecular spectrsocopic database. J Quant Spectrosc Radiat Transf 2013;130:4–50.
[35] Maki AG, Wells JS. Wavenumber calibration tables from heterodyne frequency measurements (version 1.3). Gaithersburg, MD: NIST; 1998. Available online: ⟨http://www.nist.gov/pml/data/wavenum/spectra.cfm?⟩.
[36] Saveliev VN, Ulenikov ON. Calculation of vibration–rotation line intensities of polyatomic molecules based on the formalism of irreducible tensorial sets. J Phys B: At Mol Phys 1987;20:67–83.
[37] Ulenikov ON, Sun F-G, Wang X-G, Zhu Q-S. High resolution spectroscopic study of arsine: $3\nu_1$ and $2\nu_1+\nu_3$ dyad: the tendency of symmetry reduction. J Chem Phys 1996;105:7310–5.
[38] Guelachvili G, Naumenko OV, Ulenikov ON. On the analysis of some hyperweak absorption bands of SO_2 in the regions 1055–2000 and 2200–2550 cm^{-1}. J Mol Spectrosc 1988;131:400–2.
[39] Ulenikov ON, Bürger H, Jerzembeck W, Onopenko GA, Bekhtereva ES, Petrunina OL. The ground vibrational states of PH_2D and PHD_2. J Mol Struct 2001;599:225–37.
[40] Fano U, Racah G. Irreducible tensorial sets. New York: Academic Press; 1959.
[41] Wigner EP. Quantum theory of angular momentum. New York: Academic Press; 1965.
[42] Varshalovitch DA, Moskalev AN, Khersonsky VK. Quantum theory of angular momentum. Leningrad: Nauka; 1975.
[43] Ulenikov ON, Bekhtereva ES, Albert S, Bauerecker S, Niederer HM, Quack M. Survey of the high resolution infrared spectrum of methane ($^{12}CH_4$ and $^{13}CH_4$): partial vibrational assignment extended towards 12000 cm^{-1}. J Chem Phys 2014(141): 234302_1–33.
[44] Hecht T. The vibration–rotation energies of tetrahedral XY_4 molecules. Part I. Theory of spherical top molecules. J Mol Spectrosc 1960;5:355–89.
[45] Moret-Bailly J. Sur l'interpretation des spectres de vibration–rotation des molecules a symmetrie tetraedrique ou octaedrique. Can Phys 1961;15:238–314.
[46] Champion JP. Developpement complet de l'hamiltonien de vibration–rotation adapte a l'etude des interactions dans les molecules toupies spheriques. Application aux bandes ν_2 et ν_4 de $^{12}CH_4$. Can J Phys 1977;55:1802–28.
[47] Boudon V, Champion JP, Gabard T, Loëte M, Rotger M, Wenger. Spherical top theory and molecular spectra. In: Quack M, Merkt F,

editors. Handbook of high-resolution spectroscopy, vol. 3. Wiley; 2011. p. 1437–60.
[48] Ulenikov ON, Malikova AB, Alanko S, Koivusaari M, Anttila R. High-resolution study of the $2\nu_5$ hybrid band of the CHD_3 molecule. J Mol Spectrosc 1996;179:175–94.
[49] Ulenikov ON, Bekhtereva ES, Fomchenko AL, Litvinovskaya AG, Leroy C, Quack M. On the "expanded local mode" approach applied to the methane molecule: isotopic substitutions $CH_3D \leftarrow CH_4$ and $CHD_3 \leftarrow CH_4$. Mol Phys 2014;112:2529–56.
[50] Moret-Bailly J, Gautier L, Montagutelli J. Clebsch–Gordan coefficients adapted to cubic symmetry. J Mol Spectrosc 1965;15:355–77.
[51] Rey M, Boudon V, Wenger Ch, Pierre G, Sartakov B. Orientation of $O(3)$ and $SU(2) \otimes C_I$ representations in cubic point groups (O_h, T_d) for application to molecular spectroscopy. J Mol Spectrosc 2003;219:313–25.
[52] Cheglokov AE, Ulenikov ON. On determination of the analytical formulas for reduction matrices of tetrahedral-symmetry molecules. J Mol Spectrosc 1985;110:53–64.
[53] Cheglokov AE, Saveliev VN, Ulenikov ON. Analytical representation of the values describing the spectra of T_d symmetry molecules and crystals. J Phys B: At Mol Phys 1986;19:3687–93.
[54] Tarrago G, Ulenikov ON, Poussigue G. Dipole moment matrix for vibration–rotation transitions in C_3v molecules. J Phys 1984;45:1429–47.
[55] Ulenikov ON, Bekhtereva ES, Albert S, Bauerecker S, Hollenstein H, Quack M. High resolution infrared spectroscopy and global vibrational analysis for the CH_{3D} and CHD_3 isotopomers of methane. Mol Phys 2010;108:1209–40.
[56] Nielsen HH. The vibration–rotation energies of molecules. Rev Mod Phys 1951;23:90–136.
[57] Papousek D, Aliev MR. Molecular vibrational–rotational spectra. Amsterdam, Oxford, New York: Elsevier Scientific Publishing Company; 1982.
[58] Ulenikov ON, Ushakova GA. Analysis of the H_20 molecule second-hexade interacting vibrational states. J Mol Spectrosc 1986;117:195–205.
[59] Ulenikov ON, Onopenko GA, Lin H, Zhang J-H, Zhou Z-Y, Zhu Q-S, et al. J. Mol Spectrosc 1998;189:29–39.
[60] Ulenikov ON, Onopenko GA, Tyabaeva NE, Schroderus J, Alanko S. On the rotational analysis of the ground vibrational state of CH_{3D} molecule. J Mol Spectrosc 1999;193:249–59.
[61] Ulenikov ON, He S-G, Onopenko GA, Bekhtereva ES, Wang X-H, Hu S-M, et al. High-resolution study of the $(\nu_1 1/2\nu_2\nu_3 = 13)$ polyad of strongly interacting vibrational bands of D_2O. J Mol Spectrosc 2000;204:216–25.
[62] Liu A-W, Ulenikov ON, Onopenko GA, Gromova OV, Bekhtereva ES, Wan L, et al. Global fit of the high-resolution infrared spectrum of D_2S. J Mol Spectrosc 2006;238:23–40.
[63] Ulenikov ON, Gromova OV, Aslapovskaya YS, Horneman V-M. High resolution spectroscopic study of C_2H_4: re-analysis of the ground state and ν_4, ν_7, ν_{10}, and ν_{12} vibrational bands. J Quant Spectrosc Radiat Transf 2013;118:14–25.
[64] Ulenikov ON, Gromova OV, Bekhtereva ES, Belova AS, Bauerecker S, Maul, et al. High resolution analysis of the (111) vibrational state of SO_2. J Quant Spectrosc Radiat Transf 2014;144:1–10.
[65] Ulenikov ON, Gromova OV, Bekhtereva ES, Fomchenko AL, Sydow C, Bauerecker S. First high resolution analysis of the $3\nu_1$ band of $^{34}S_2^{16}$. J Mol Spectrosc 2016;319:50–4.
[66] Wenger C, Boudon V, Rotger M, Sanzharov M, Champion J-P. XTDS nd SPVIEW: graphical tools for the analysis and simulation of high-resolution molecular spectra. J Mol Spectrosc 2008;251:102–13.
[67] Tarrago G, Ulenikov ON, Poussigue G. Dipole moment matrix for vibration–rotation transitions in C_3v molecules. J Phys 1984;45:1429–47.
[68] Saveliev VN, Ulenikov ON. Calculation of vibration–rotation line intensities of polyatomic molecules based on the formalism of irreducible tensorial sets. J Phys B: At Mol Phys 1987;20:67–83.